*Graphical Abstract

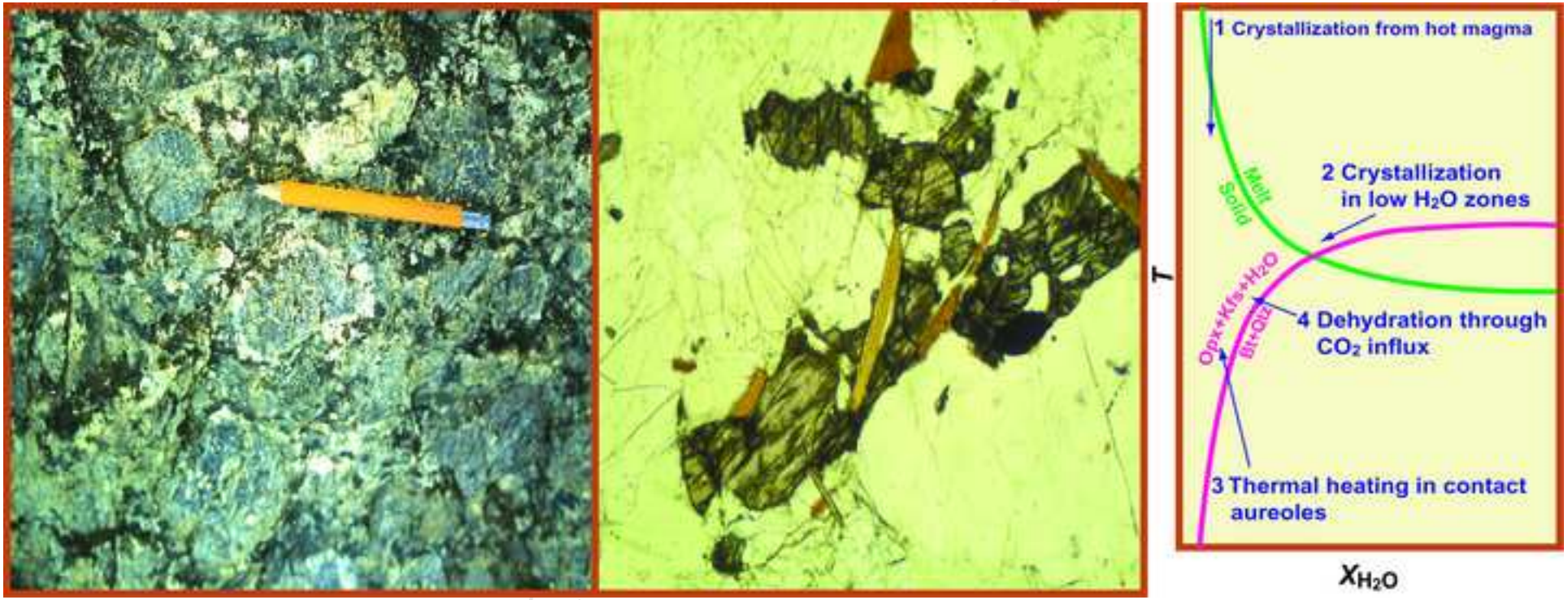

Multiple origins of charnockite in the Mesoproterozoic Natal belt, Kwazulu-Natal, South Africa

G.H. Grantham[a,*], P. Mendonidis[b], R.J. Thomas[c], M. Satish-Kumar[d]

Four charnockite genetic models from the Natal belt are described, two of which have not previously been formally described in the literature.

New C isotope data indicate a mantle origin for the CO_2 inclusions previously reported from the magmatic charnockitic Port Edward Pluton.

Multiple origins of charnockite in the Mesoproterozoic Natal belt, Kwazulu-Natal, South Africa

G.H. Grantham[a,*], P. Mendonidis[b], R.J. Thomas[c], M. Satish-Kumar[d]

[a] *Central Regions Unit, Council for Geoscience, P/Bag X112, Pretoria, South Africa*

[b] *Vaal University of Technology, Andries Potgieter Boulevard, Vanderbijlpark, South Africa*

[c] *British Geological Survey, Keyworth, Nottingham, NG12 5EQ, UK*

[d] *Institute of Geosciences, Faculty of Science, Shizuoka University, 836 Oya, Suruga-ku, Shizuoka, 422-8529, Japan*

* corresponding author:

Email address: grantham@geoscience.org.za

Received 1 December 2011; Received in revised form 20 April 2012; accepted 24 May 2012

Abstract Four different varieties of charnockitic rocks, with different modes of formation, from the Mesoproterozoic Natal belt are described and new C isotope data presented. Excellent coastal exposures in a number of quarries and river sections make this part of the Natal belt a good location for observing charnockitic field relationships. Whereas there has been much debate on genesis of charnockites and the use of the term charnockite, it is generally recognized that the stabilization of orthopyroxene relative to biotite in granitoid rocks is a function of low aH_2O (± high CO_2), high temperature, and composition (especially Fe/(Fe+Mg)). From the Natal belt exposures, it is evident that syn-emplacement, magmatic crystallization of charnockite can arise from mantle-derived differentiated melts that are inherently hot and dry (as in the Oribi Gorge

granites and Munster enderbite), as well as from wet granitic melts that have been affected through interaction with dry country rock to produce localized charnockitic marginal facies in plutons (as in the Portobello granite). Two varieties of post-emplacement sub-solidus charnockites are also evident. These include charnockitic aureoles developed in leucocratic, biotite, garnet granite adjacent to cross-cutting enderbitic veins that are attributed to metamorphic-metasomatic processes (as in the Nicholson's Point granite, a part of the Margate Granite Suite), as well as nebulous, patchy charnockitic veins in the Margate Granite that are attributed to anatectic metamorphic processes under low-$a$$H_2O$ fluid conditions during a metamorphic event. These varieties of charnockite show that the required physical conditions of their genesis can be achieved through a number of geological processes, providing some important implications for the classification of charnockites, and for the interpretation of charnockite genesis in areas where poor exposure obscures field relationships.

Key Words: Charnockite igneous; Metamorphic; Natal belt; Dehydration CO_2

1. Introduction

Charnockitic rocks are broadly defined as granitoids in terms of Quartz-Alkali feldspar-Plagioclase (QAP) ternary space but contain orthopyroxene (or fayalite + quartz) and, typically, perthite, mesoperthite or antiperthite (Le Maitre, 2002). Although not included in the formal definition, charnockitic rocks are typically characterized by meso- to melanocratic colour indices, being commonly described as having a "dark green, greasy" lustre and in contrast to the

leuco appearance normally expected of granitoids. The stabilization of orthopyroxene in granitic rocks and quartzofeldspathic granulites in high grade terrains essentially requires low aH_2O and/or high temperatures typical of granulite grade environments. If aH_2O is high, then typically orthopyroxene is replaced by biotite or amphibole, either in the solid state or as crystallizing phases in the melt at appropriate temperatures. The genesis of charnockitic rocks was widely debated during the 80's and 90's with numerous models revolving around the modes of genesis between magmatic and metamorphic varieties and the distinction of these (e.g. Bohlender et al., 1992) and particularly in the role of CO_2 in the fluid phase (Newton et al., 1980; Friend, 1981; Janardhan et al., 1981; Kumar, 2004; Santosh and Omori, 2008; Huizenga and Touret, 2012; Touret and Huizenga, 2012). Carbon isotopic composition of fluid inclusions and graphite have served as distinct markers in identifying the mantle signatures of carbonic fluids in many occurrences of charnockite formation (e.g. Jackson et al., 1988; Farquhar and Chacko, 1991; Santosh et al., 1991; Luque et al., 2012).

A number of variations of these genetic models have been put forward over the years, including:

- Primary magmatic charnockite generated, with the crystallization of orthopyroxene, from high temperature magmas with low aH_2O (Saxena, 1977; Martignole, 1979; Wickham, 1988; Stern and Dawoud, 1991; Kilpatrick and Ellis, 1992).
- Magmatic charnockite generated by the melting of granulites at high pressures in the presence of a carbon dioxide-rich fluid phase (Wendlandt, 1981).
- Metamorphic charnockites which are anhydrous restites of lower crust material from which partial melts have been removed (Fyfe, 1973; Newton and Hansen, 1983; Clemens, 1992).
- Metamorphic charnockites formed during granulite grade metamorphism under fluid

conditions of low oxygen fugacity and high partial pressures of carbon dioxide involving the breakdown of hydrous mafic phases and the generation of orthopyroxene (Janardhan et al., 1979; Newton et al., 1980; Friend, 1981; Hansen et al., 1984; Hansen et al., 1987; Hansen et al., 1995).

- Metasomatic charnockites formed by the dehydration of hydrous minerals by brines (Perchuk and Gerya, 1993; Aranovich and Newton, 1995).
- Metamorphic charnockites formed by thermal desiccation in aureoles adjacent to hot anhydrous intrusions emplaced into granitic rocks (van den Kerkhof and Grantham, 1999).

Each of these mechanisms contributes to the fundamental requirements of high temperatures and low $a\mathrm{H_2O}$ for charnockite genesis. However, since many of these examples occur in isolation, the interpreted mechanism was often extrapolated as the mechanism of formation of all charnockites, hence the debates. Many of the debates have since subsided with little resolution of the matter except to accept that multiple origins of orthopyroxene-bearing granitoid rocks are recognized.

Charnockitic rocks from the southern portion of the Mesoproterozoic (ca. 1.2 to 1.0 Ga) Natal belt of KwaZulu-Natal, South Africa (Fig. 1), were first reported by Gevers (1941) and Gevers and Dunne (1942). The original mapping of this area was done by du Toit (1946) and later McIver (1963, 1966) provided a regional study of the area and described the major lithologies. Subsequently, we have recognized four distinct types of charnockite genesis in the area, comprising two magmatic and two metamorphic varieties. The description of these varieties and their interpreted genetic environments are the topic of this paper, supported by new C isotope data from some of the localities.

2. Natal Metamorphic Province

The Natal Metamorphic Province ("Natal belt" for short) consists of three tectonic terranes (Thomas, 1989; Fig. 1). A summary of the lithologies for which emplacement ages have been reported is depicted in Fig. 2, which shows that the Natal belt has a tectonomagmatic history spanning a period of time from >1200 Ma to ~1026 Ma. Geochemical data from lithologies from all three terranes (Thomas et al., 1994; Arima et al., 2001; Mendonidis et al., 2009) suggest island arc leading to the interpretation that the terranes were island arcs accreted onto the southern margin of the Archaean Kaapvaal Craton (Jacobs et al., 1993; Arima et al., 2001; McCourt et al., 2006).

The northernmost Tugela Terrane comprises plutonic, volcanic and sedimentary rocks that were obducted onto the southern margin of the Kaapvaal Craton, which they now overlie (Matthews, 1972; Barkhuizen and Matthews, 1990; Johnston et al., 2003). The southern margin of the Tugela Terrane is marked by the Lilani-Matigulu shear zone (Thomas, 1989).

The Mzumbe Terrane covers a large area south of the Lilani-Matigulu shear zone, and comprises supracrustal gneisses, dated at ca. 1230 Ma (Thomas et al., 1999), which were intruded by a wide range of meta-igneous rocks including TTG orthogneisses and later gabbros (Thomas, 1989; Thomas and Eglington, 1990). The Mzumbe Terrane is separated from the southernmost Margate Terrane by the Melville thrust. The southernmost Margate Terrane consists of paragneisses intruded by calc-alkaline and tholeiitic, mafic to intermediate meta-igneous suites and a number

of granitic sheets and plutons (Talbot and Grantham, 1987). Large plutons of a rapakivi-charnockitic association collectively called the Oribi Gorge Suite (Thomas, 1988a, b; Thomas et al., 1993a; Grantham et al., 2001; Eglington et al., 2003) punctured both the Margate and Mzumbe Terranes between 1090–1025 Ma (Fig. 2) indicating that these two terranes were juxtaposed by that date (Thomas, 1989; Eglington et al., 2003; Eglington, 2006).

All three terranes experienced multiple deformational events and are characterized by pervasive E-W trending fabrics and northward-verging overall structure (Talbot and Grantham, 1987; Mendonidis and Strydom, 1989; Thomas, 1989; Jacobs et al., 1993; McCourt et al., 2006; Bisnath et al., 2008). However, the timing of the events in the different terranes was not coeval as shown in Fig. 2. Multiple metamorphic events have been reported from each terrane and metamorphic textures suggest that metamorphism coincided with the deformation events (Mendonidis, 1989; Mendonidis et al., 2002; Mendonidis and Grantham, 2003; Bisnath et al., 2008). Metamorphic grade generally increases from greenschist facies in the north to granulite facies in the south (Matthews, 1972; Thomas et al., 1994; McCourt et al., 2006).

The earliest recognition and descriptions of charnockite in the Natal belt were by Gevers and Dunne (1942) and McIver (1963, 1966). Local, but excellent exposures, mostly above and in the intertidal zone along the coast, have facilitated the recognition of the various types of charnockite described here, making the Natal Metamorphic Province an almost unique area to study charnockite genesis, even by comparison with the classic charnockite areas of southern India.

3. Magmatic charnockites

The magmatic charnockites in the Natal belt are related to three distinct plutonic igneous rock units: the Oribi Gorge Suite (OGS) (Thomas, 1988a, b; Thomas et al., 1991), the Munster Suite (Mendonidis and Grantham, 1989, 1990) and the Margate Granite Suite (Thomas et al., 1991) (Figs. 1 and 3). Within these intrusive suites, two charnockite varieties are distinguished based on the dominant controlling factors of their genesis, namely fractionational crystallization and fluid activity.

3.1 *Charnockites with evidence of magmatic crystallization*

Two chemically distinct plutonic suites of megacrystic granitoids are recognized in the Natal belt namely the Oribi Gorge Suite and the Munster Suite. The Oribi Gorge Suite contains the most extensive development of charnockites in the Natal belt, where it is restricted to the Margate and Mzumbe Terranes in the southern part of the belt (Thomas, 1988b, 1989; Fig. 1). The Oribi Gorge Suite was intruded between ca. 1090 and 1025 Ma (Eglington et al., 2003). It is made up of ten major plutons (up to 750 km^2 in extent), consisting of very coarse-grained, feldspar porphyritic, locally rapakivi-textured, granitoid and charnockite. Eglington et al. (2003) provided U-Pb SHRIMP ages for some of the plutons as follows: Two samples from the Oribi Gorge plutons provided magmatic ages of 1082 ± 7 Ma and 1064 ± 5 Ma and a metamorphic rim age of 1029 ± 8 Ma, and the Fafa and Port Edward plutons provided ages of 1037 ± 10 Ma and 1025 ± 8 Ma respectively. These data suggest two episodes of intrusion at ~1070 and 1030 Ma (Eglington et al., 2003). Intrusions in which charnockitic rocks are known to be developed include the Port Edward, Oribi Gorge, Ntimbankulu, Fafa, KwaLembe, Mgeni and Glendale

plutons (Fig. 1). Some intrusions contain very little charnockite (e.g. the Mvenyane pluton), whereas others are exclusively charnockitic (e.g. the Port Edward pluton). In the Oribi Gorge Suite, a primary igneous flow fabric, formed by sub-parallel alignment of tabular feldspar phenocrysts, can be seen locally in low-strain zones. Elsewhere, a weak to strong regional S_2 fabric is developed, giving a pronounced gneissic foliation, especially around and parallel to pluton margins where augen gneisses locally predominate. Pluton cores may contain low-strain zones devoid of a tectonic fabric, though many are deformed by later ductile, transcurrent shears which produced extensive, west-trending, sub-vertical augen gneiss and mylonite belts (Thomas, 1989; Thomas et al., 1991). The Oribi Gorge Granitoid Suite is characterized by megacrystic (up to 6 cm) subhedral to euhedral feldspar grains with interstitial quartz, ferromagnesian and accessory minerals (Fig. 4A). The ratio of K-feldspar and plagioclase is variable, so that within a single pluton the normal granitic (charnockitic) composition grades to granodiorite (enderbite) with increasing plagioclase, or monzonite/quartz monzonite (mangerite/mangeronorite) with decreasing quartz. Rapakivi textures are locally recognizable in some plutons (Fig. 4C). The Oribi Gorge charnockites (sensu lato) are typically very dark green to black in colour, have a resinous lustre and consist of perthitic K-feldspar and/or antiperthitic plagioclase phenocrysts in enderbitic rocks. The coarse-grained groundmass is composed of quartz (8%–30%), antiperthitic plagioclase (An_{25}; 25%–60%) and subordinate microcline or orthoclase (12%–45% + myrmekite). Mafic minerals, which form interstitial aggregates, include brown/brownish-green hornblende (~5%), reddish-brown biotite (0–5%; locally symplectically intergrown with quartz), weakly pleochroic orthopyroxene (5%–15%) ± pale-green clinopyroxene (0–5%), partially altered fayalite (0–5%) and late garnet (up to ~5%; commonly in garnet-quartz symplectite). Accessory minerals include sulphides, ilmenite, zircon, apatite, allanite and graphite. Apatite,

ilmenite and zircon commonly occur as inclusions in interstitial ferromagnesian minerals suggesting late crystallization. Olivine grains are locally mantled by orthopyroxene suggesting the following reaction: fayalite + quartz → orthopyroxene (Grantham et al., 2001).

The geochemistry from the various intrusions has been described and discussed in Grantham (1984), Kerr (1985), Eglington et al. (1986), Thomas (1988b), Thomas and Mawson (1989) and Grantham et al. (2001). The Oribi Gorge Suite is typically tholeiitic with high FeO/(FeO+MgO (Fig. 5) and shows A-type, within plate- and rapakivi-granite geochemical characteristics (Thomas, 1988b). K_2O, Na_2O, FeO and P_2O_5 are high for average granitoids with comparable silica contents. (Na_2O+K_2O)/CaO ratios, TiO_2 and P_2O_5 contents are high. Trace element abundances are also typical of A-type granitoids, with high contents of the HFS elements Nb, Y, Zr and Ba. Within individual plutons, major and trace element distributions show strong linear trends on Harker diagrams. The least evolved of the plutons, the Port Edward pluton has marginal contact phases with relatively low SiO_2 contents of ~53% (Grantham, 1984), typical of basic rocks, albeit with a high Fe/(Fe+Mg) ratio.

The geology and geochemistry of the Munster Suite has been described in detail by Mendonidis and Grantham (1989, 1990) and has an age of ~1092 Ma (Mendonidis et al., 2009) indicating it is older than the Oribi Gorge Suite. The Munster Suite comprises older mafic granulites and younger intermediate charnockites. The older generation of coarse- to fine-grained, mafic rocks contain plagioclase, two pyroxenes, biotite, minor K-feldspar ± hornblende and quartz. The younger, coarse-grained charnockitic generation is quartz-monzonitic in composition and consists of quartz, K-feldspar, plagioclase, orthopyroxene, clinopyroxene, biotite, opaque

mineral and apatite. These rocks are typically characterized by megacrystic (2–3 cm) plagioclase with interstitial quartz, ferromagnesian phases and accessory minerals, Mendonidis (1989) recognized two generations of orthopyroxene in these rocks; an earlier magmatic variety and later metamorphic pyroxene derived from biotite and hornblende. The suite defines a calc-alkaline trend and the rocks are characterized by high TiO_2 and P_2O_5 contents (Fig. 5). Mendonidis and Grantham (1989) concluded that the basic and intermediate components of the Munster Suite were co-genetic.

Two pyroxene geothermometry on the basic rocks of the Munster Suite (after Lindsley, 1983), using mineral core compositions, yielded magmatic temperatures of ~1050 °C, whereas rim compositions suggest far lower temperatures of ~600 °C, reflecting metamorphic cooling or closure temperatures (Mendonidis and Grantham, 1989). This interpretation is supported by the occurrence of oscillatory zoning in clinopyroxene cores, interpreted as relict igneous features. Conversely, no oscillatory zoning is seen in adjacent orthopyroxene, which is interpreted as a metamorphic rather than an igneous phase. Furthermore, petrographic textures indicate that orthopyroxene developed at the expense of biotite and hornblende during prograde metamorphism from amphibolite to granulite facies (Grantham, 1984).

Evidences for very high temperatures of ~1000 °C in the Port Edward pluton of the Oribi Gorge Suite are derived from two pyroxene thermometry reported in Grantham et al. (2001). Saturation surface thermometers based on the solubility studies of Zr and P_2O_5 (Watson, 1979; Watson and Pabianco, 1981; Watson and Harrison, 1983) in granitic melts using available whole rock chemistry (Grantham 1984; Mendonidis and Grantham, 1989) support high crystallization

temperatures. P_2O_5 and Zr contents of the Port Edward pluton suggest temperatures of 1000–1050 °C and ~825–925 °C respectively whereas the data from the Munster Suite suggest temperatures of 975–1025 °C and 825–850 °C respectively (Fig. 5). Similarly comparison of the TiO_2 contents of these rock units with the solubility data of TiO_2 of Green and Pearson (1986) suggest temperatures of 1000–1050 °C and ~950 °C for the Port Edward pluton and Munster Suites respectively (Grantham et al., 2001 and Fig. 5).

Another group of rocks with magmatic charnockitic affinity is the Turtle Bay Suite, an undated meta-igneous association intruded along the tectonic boundary between the Mzumbe and Margate terranes. The suite comprises a mantle-derived assemblage of mafic two-pyroxene granulites and fractionated enderbites metamorphosed under granulite facies conditions of ca. 850 °C and ca. 6 kb (Thomas et al., 1992).

Radiogenic isotope data (Sm/Nd and Rb/Sr) indicate that the Oribi Gorge Suite is juvenile with Sm/Nd and Rb/Sr data showing no significant contributions from older crust (Eglington et al., 1986; Grantham et al., 2001). No radiogenic isotope data are available from the Munster Suite. Fluid inclusion studies on the Port Edward pluton reveal high density CO_2 inclusions with subordinate N_2 and CH_4 contents (Van der Kerkhof and Grantham, 1999).

To further understand the genesis of these rocks and the source of the CO_2, which is present in high levels in fluid inclusions (along with native graphite in the OGS charnockites) a carbon isotope study was conducted on samples from the Port Edward and Oribi Gorge plutons. Sample preparation and cleaning procedures followed the methods described in Miller and Pillinger

(1997). Bulk rock and mineral separates of 0.5 to 1 mm in size were hand-picked under a binocular microscope for the extraction of fluid inclusions by the heating method. Samples were treated with hot 6 M HCl to remove any surficial carbonate contaminants and washed in distilled water. Subsequently, the samples were ultrasonically cleaned in dichloromethane. Prior to extraction, 1 to 2 g of mineral separate was loaded into preheated (1100 °C, 12 h) 9 mm quartz tubes and heated at 500 °C overnight to remove any surface and organic contaminants. An oxidizing agent (V_2O_5) was added to one aliquot each of bulk sample to check whether small amounts of CH_4 or graphite are present, which can affect the isotopic composition (Satish-Kumar, 2005). The quartz tubes were then sealed under high vacuum and heated to 800 °C or 1000 °C and released gases were cryogenically purified and CO_2 was separated, and analyzed for its carbon isotope composition using a MAT-250 mass spectrometer at Shizuoka University, Japan. CO_2 blanks during the heating experiments were always less than 0.005 mol.

The results of carbon isotopic composition of CO_2 extracted from fluid inclusions in two representative samples are given in Table 2. The whole rock samples gave slightly lower $\delta^{13}C$ values at 1000 ºC, when compared to those at 800 ºC. This trend is again observed in CO_2 extracted in samples with oxidizing agent, which implies that at 1000 ºC there is a possibility that CO_2 was partly derived from the oxidation of small amounts of graphite. Graphite can be deposited inside the fluid inclusions or in mineral grain boundaries during retrogression from CO_2-rich fluids (e.g.Van der Kerkhof et al., 1991; Satish-Kumar, 2005; Papineau et al., 2010) and is a primary constituent of some of the charnockites (Thomas, 1988b). Furthermore, minerals like quartz are vulnerable for secondary fluid inclusion entrapment and it is difficult to separate primary and secondary fluid inclusions with heat extraction. The samples were pre-heated at 500

ºC to decrepitate all possible low temperature secondary fluids. Therefore, the carbon isotopic composition of CO_2 extracted from fluid inclusions at 800 ºC is considered as the best approximate values for the fluid inclusions. The carbon isotopic composition of fluid inclusions in both charnockite samples gave values comparable to mantle derived carbon (Table 2), which is reported to have $\delta^{13}C$ values around –5.5‰ (Mattey, 1991; Deines, 2000). These values are also comparable with the fluid inclusion carbon isotope data described in southern Indian charnockite, which envisages a deep crustal or mantle source (e.g. Jackson et al., 1988; Santosh et al., 1991). Significant differences between the quartz and whole rock values may reflect additional C bearing phases (carbonates?) in the whole rocks.

Recognizing the basic composition of some of the samples of the Oribi Gorge Suite (with SiO_2 contents of <55% in, for example the Port Edward pluton) and the Munster Suite, their high temperatures of crystallization of ~950–1050 °C, indicated by two pyroxene thermometry and saturation surface thermometry, and the juvenile radiogenic and stable isotope data from the Oribi Gorge Suite, it is concluded that the magmas from which these rocks crystallized were mantle derived. The original magmas were probably basaltic in origin. In the case of the Port Edward pluton and probably the Oribi Gorge Suite in general, the magmas may have undergone two phases of crystallization with earlier crystallization at depth resulting in typical tholeiitic Fe/(Fe+Mg) enrichment before emplacement and continued fractional crystallization at higher crustal levels. In contrast, basic members of the Munster Suite are recognized at the current levels of exposure (Mendonidis and Grantham, 1989). The two suites are genetically distinct; the Oribi Gorge Suite including the Port Edward Pluton has Fe/(Fe+Mg) ratios of ~0.75 and the Munster Suite an Fe/(Fe+Mg) ratio of ~0.6 (Figs. 5 and 6 in Grantham et al., 2001).

The overall texture of the megacrystic charnockites of the Munster and Oribi Gorge Suites may also be interpreted in terms of experimental work by Wyllie et al. (1976) and Naney (1983), Whitney (1975) and Naney and Swanson (1980), who demonstrated that in granitic and granodioritic magmas, under conditions of reduced or low $p(H_2O)$ ($w(H_2O)$ <4.5%), plagioclase and alkali feldspar are early phases on the liquidus and commonly precede the crystallization of quartz and ferromagnesian phases (typically hornblende or orthopyroxene). In granodioritic systems with $w(H_2O)$ >4.5%, on the other hand, hornblende is typically the first liquidus phase. Concomitant with low $p(H_2O)$ is the need for high magmatic temperatures of the order of ~1000 °C. The inferred crystallization path of these rocks is shown in Fig. 6. The path shows early crystallization of megacrystic plagioclase on the liquidus followed by orthopyroxene. Later as the K-feldspar field is crossed separate grains of orthoclase or as rapakivi overgrowths on plagioclase are formed with later interstitial or intercumulate orthopyroxene, opaque oxides and accessory phases zircon and apatite. The crystallization sequence will vary also due to changes in residual bulk composition with fractionation. The inferred crystallization sequence is reflected in Fig. 4B which shows a ~1 cm plagioclase grain rimmed by quartz, ilmenite and poikilitic orthopyroxene and clinopyroxene grains, all of which contain inclusions of apatite and zircon. These inclusions indicate crystallization after the feldspars but preceding the pyroxene and ilmenite and imply near saturation of Zr, P_2O_5 and TiO_2 in the melt.

3.2 Magmatic fluid activity charnockites in the Portobello Granite

A second generation of leucocratic magmatic charnockites, with granitic (sensu stricto) composition, is recognized in the southern Margate Terrane of the Natal belt (Thomas, 1988a).

These charnockites are associated with non-charnockitic, often garnetiferous leucogranites. One body, the Portobello Granite shows both charnockitic and non-charnockitic facies. The non-charnockitic variety is typically a red-coloured, biotite-chlorite granite exposed at the Portobello headland and along Palm Beach (Figs. 3, 4d and 7) in which chlorite post-dates and mostly replaces biotite, indicative of later, low-temperature alteration (Fig. 8a, b). There are also rare chlorite grains which may be pseudomorphs after orthopyroxene, but no preserved orthopyroxene has been recognized in the pink granite. Unequivocal contact relationships show that the Portobello Granite intruded quartz monzonorites and metabasites of the Munster Suite (Fig. 7). Wherever the granite is in contact with the quartz monzonorites, it is characterized by a 0.5 to 1.5 m wide grey-coloured, charnockitic marginal phase that contains biotite and orthopyroxene as mafic phases (Figs. 4d and 8c, d). The charnockitic margins show a much lower degree of chlorite alteration than the rest of the granite. A U-Pb zircon (SHRIMP) discordant intercept age of 1057 ± 27 Ma was determined for the main body of red-coloured biotite-chlorite granite of the Portobello Granite from metamict zircon grains (Mendonidis and Armstrong, 2009). The metamict nature of the zircons may be related to low temperature alteration. Zircons from the charnockitic margins, on the other hand, produced a near-concordant age of (1093 ± 7) Ma that is statistically identical to the age of the adjacent Munster Suite quartz monzonoritic country rocks (1091 ± 7 Ma) (Mendonidis and Armstrong, 2009; Mendonidis et al., 2009). The zircons from the charnockitic margins were pristine, clear, transparent, light-brown grains distinctly different from the milky, metamict grains of the rest of the granite, and resembled those from the quartz monzonorites country rocks. Therefore, the zircons from the charnockitic margins were interpreted as being xenocrysts derived from the partial assimilation of the quartz monzonoritic country rocks (Mendonidis and Armstrong, 2009).

In comparison to the granite, the charnockitic margins are depleted in K, Rb, P, Y, Nb and REE, and enriched in Ca, Ba and Sr (Mendonidis and Grantham, 2000, 2005; Table 3, Fig. 9). The depletion of K and Rb in the marginal zones is inferred to be due to the migration of these hydrophilic elements with the fluid into the country rock where they facilitated retrograde alteration of orthopyroxene to biotite and/or to reduced crystallization of primary biotite in the contact zone with Rb being typically strongly partitioned into K feldspar. The hydrous fluid may also have fluxed melting reactions in the quartz monzonorite involving the breakdown of plagioclase allowing partial assimilation, thus explaining the enrichment in Ca, Ba, and Sr in the charnockitic margins. Phosphorous is relatively insoluble in felsic melts (Harrison and Watson, 1984) and may have precipitated and nucleated onto existing apatite in the country rock. The depletion of Nb, Y and the REE can also be accounted for in terms of their being preferentially partitioned into apatite in the quartz monzonoritic country rock.

An interpretation that accounts for all the observed features noted above is that the Portobello Granite intruded as a wet felsic magma into the dry quartz monzonorite. On solidification, the water that was dissolved in the melt remained as a hydrous fluid that promoted chloritic alteration of the mafic phases in the granite. In the marginal zones, the fluid migrated along a fluid gradient into the dry country rock, leaving the marginal zones relatively dry and thus limiting retrograde alteration. This relationship is reflected in Fig. 10 in which the solidus curve for wet granite is shown along with two curves for the dehydration reaction of Bt + Qtz → Kfs + Opx + H_2O with the two curves reflecting Mg and Fe end members (Mineral abbreviations after Kretz, 1983). The two horizontally oriented arrows on Fig. 10 for the two curves show how with

a decreasing H_2O fluid gradient, it would be possible to contribute to orthopyroxene crystallization/stabilization near the contact of the intrusion with dry country rock.

4. Metamorphic charnockites

In addition to the charnockites which we interpret as of magmatic origin, as discussed above, two varieties of metamorphic charnockite, hosted in the Margate Granite Suite are recognized. The two types are further subdivided on the basis of the dominant controlling factor of their genesis namely, "thermal metamorphic charnockite" or "aureole charnockite" and "metamorphic fluid activity charnockite".

4.1 Thermal metamorphic charnockite ("aureole charnockite")

This variety of charnockite is recognized in the Nicholson's Point granite, a leucocratic biotite garnet granite and a member of the Margate Granite Suite, and has been described in detail by Grantham et al. (1996) and Van der Kerkhof and Grantham (1999). The critical exposures are seen at Nicholson's Point (Fig. 11). At this locality the country rock Nicholson's Point granite is intruded by veins of Port Edward Enderbite (Oribi Gorge Suite magmatic charnockite) up to ~10 m thick as well as by pegmatitic veins up to ~30 cm wide. Adjacent to the veins of Port Edward enderbite, charnockitic aureoles with diffuse margins up to ~4 m wide are developed in the leucocratic biotite garnet Nicolson's Point granite (Figs. 4A and 11). Aureoles in the granite adjacent to pegmatite veins are up to 0.5 m wide with aureole/vein width ratios ~10:1 (Fig. 4E) (Van der Kerkhof and Grantham, 1999).

The medium- to coarse-grained Nicholson's Point granite is a leucogranite composed of anhedral granoblastic orthoclase, plagioclase, quartz, biotite and garnet with accessory pyrite, ilmenite, zircon and apatite. The charnockitic phase contains hypersthene (Fig. 8g, h), less biotite, but more plagioclase, myrmekite and opaque minerals relative to the granite. The sulphide in the charnockite is pyrrhotite rather than pyrite. Garnet occurs both in the leucogranite and the charnockite, either as euhedral to subhedral inclusion-free crystals (Fig. 8e, f) or as xenomorphic poikilitic grains in symplectic intergrowth with quartz. The former generation is restricted to the granitic phase in which it occurs as isolated grains, commonly enclosed within feldspars and is interpreted as a primary igneous phase (Van der Kerkhof and Grantham, 1999). The garnet-quartz symplectites occur adjacent to opaque minerals and around hypersthene in the charnockitic phase and are interpreted to represent isobaric cooling reactions of Opx/Mt + Pl → Grt + Qtz (Van der Kerkhof and Grantham, 1999). Where the two generations are in contact, the symplectic garnet is seen to post-date the inclusion-free variety. Biotite is randomly distributed in the leucogranite, but occurs in association with mafic and opaque minerals in the charnockite. This is interpreted as partial retrogressive hydration (Fig. 8g, h).

The same phenomenon is seen on a regional scale, where similar variations are observed involving granites of the Margate Granite Suite comprising leucocratic pale grey to cream-coloured garnetiferous granite with dark greyish green charnockite (Fig. 3; Thomas, 1988a; Thomas et al., 1991) forming discontinuous, non-pervasive large-scale aureoles (> 1 km wide) around plutons of the Oribi Gorge Suite (Fig. 3).

Thermobarometry and fluid inclusions studies were completed on the Nicholson's Point granite to investigate the causes of the charnockitisation. The minimum temperature conditions for the charnockite forming reaction were constrained by the breakdown of pyrite to pyrrhotite at ~700 °C, recognizing that the enderbite intruded with a temperature of ~900–1000 °C. Thermobarometry using compositional data from coexisting garnet and orthopyroxene yielded lower unrealistic temperature estimates which were interpreted to represent cooling temperatures (Van der Kerkhof and Grantham, 1999).

Fluid inclusions studies of the rock units involved in this process showed that the intruding hot Port Edward enderbite was characterized by dense CO_2 and N_2 fluid inclusions, the metamorphic aureole by virtually pure H_2O inclusions, whereas the country rock Nicholson's Point granite was characterized by saline H_2O inclusions (Van der Kerkhof and Grantham, 1999). These differences indicate that the charnockitic aureoles were not the result of CO_2 causing a reduction in the aH_2O and stabilizing Opx and indicating a different mechanism for genesis. The densities of the H_2O-rich inclusions in the charnockite showed a wide range which was interpreted to reflect re-equilibration and implosion during the isobaric cooling path inferred in the area (Van der Kerkhof and Grantham, 1999). In contrast, the CO_2 inclusions in the intruding enderbite showed a limited density range consistent with their entrapment at high temperatures of crystallization. The survival of these inclusions was attributed to the isochores for CO_2 inclusions having shallower slopes and consequently being closer to the isobaric cooling path inferred for the area (Van der Kerkhof and Grantham, 1999).

Even though the charnockitisation occurred at temperatures >700 °C the Nicholson's Point granite country rock did not melt because it was virtually anhydrous. The granite contains only ~5% biotite, containing a maximum of ~4% stoichiometric H_2O, so the amount of H_2O released from the biotite breakdown reaction Bt + Qtz → Opx + Kfs +H_2O was only ~0.2% of the rock by volume (Van der Kerkhof and Grantham, 1999). The effect of the low aH_2O is summarized in Fig. 10. The vertical double-headed arrow on the figure defines the trajectory of the charnockite forming reaction showing the crossing of the Bt + Qtz →Opx + Kfs + H_2O reaction curve with increasing temperature with the production of pyroxene in the solid state.

No significant differences are evident in the major element chemistry between the leucogranite and the charnockite phases of the Nicholson's Point granite, showing that the process is essentially isochemical (Fig. 12). However, Grantham et al. (1996) noted that the charnockite is slightly depleted in Rb, Th, Nb, Y and REE (except Eu) whereas the charnockite is enriched in S, Ba and Sr (Fig. 12).

The chemical variations are consistent with a combination of trace elements being incompatible in the products of the charnockite-forming reaction and metasomatic introduction of mobile elements from the intruding magma. Depletions in the charnockite of Rb, Th, and Nb are correlated with biotite being replaced by orthopyroxene whereas the REE depletions are correlated with the replacement of garnet by pyroxene recognizing that the REE are preferentially partitioned into garnet and Rb, Th and Nb being preferentially partitioned into biotite (Grantham et al., 1996). The higher S, Ba and Sr are interpreted to be metasomatic introductions from the enderbite.

The discontinuous regional charnockite developed in the leucogranitic country rocks of the Margate Granite Suite adjacent to magmatic charnockite intrusions thus probably represent large-scale thermal aureoles in which biotite was dehydrated to form hypersthene and garnet was altered to hypersthene. No *p-T* studies have been done to understand the physical conditions with such studies being dependant on identifying methods independent of fluid content and not affected by subsolidus cooling and exchange. Charnockite aureoles adjacent to pegmatites show identical geochemical features to those around enderbites. However, in view of the high aureole/vein width ratio, they could not have developed as a result of high temperatures and it is suggested that the charnockite-forming reaction in this case was fluid driven with the pegmatite providing a sustained, possibly hypersaline, fluid source (Aranovich and Newton, 1995).

4.2 Metamorphic fluid activity charnockite (fluid-induced charnockitisation)

Vein-like and nebulous patches of coarse-grained charnockite have been described from southern Natal (Thomas, 1988a). These resemble in appearance the well-documented "arrested charnockites" of the Kerala region of southern India (e.g. Allen et al, 1985; Kumar, 2004; Raith and Srikantappa, 2007) and like most of those, they post-date the metamorphic fabric and appear to have originated by the introduction of fluids (Saunders, 1995).

In southern Natal, these charnockitic zones occur within the granite-gneisses of the Margate Suite and Glenmore Granite, mostly in a wide belt around the southern margin of the Oribi Gorge Pluton and close to the high-grade marbles of the Marble Delta Formation of the

Mzimkulu Group (Thomas, 1988a; Fig. 3). The granites of both the Margate Suite and Glenmore Granite are strongly foliated and locally preserve evidence of two fabrics (Talbot and Grantham, 1987; Mendonidis and Strydom, 1989). They both have S-type chemical characteristics (Mendonidis et al., 1991; Thomas et al., 1991) and may be interpreted as having originated by fluid absent melting of metasediments (of the Mzimkulu Group?) during the high temperature-low pressure D1 (S1, M1) granulite event recognized by Mendonidis and Grantham (2003). Both these granites contain garnetiferous and charnockitic leucosomes that are concordant to the S2 fabric, and probably originated through syn-M2 fluid-absent anatexis (Saunders, 1995).

Post-S2 vein and patch charnockites crop out at two quarries in the northern part of the Margate Terrane (Thomas, 1988a; Fig. 3). They are composed of typical, rather heterogeneous Margate Suite garnet leucogranite and augen gneiss and are cut by a number of discordant charnockite veins (Fig. 3; Thomas, 1988a). The charnockites in the two quarries were described in detail and interpreted by Saunders (1995). The distribution of the discordant pegmatitic charnockitic veins is controlled by small ductile shear zones with predominantly sinistral displacements. The host-vein boundary is typically sharp and marked by a five-fold grain-size increase from ~0.5–2.5 mm and a colour change from the light grey leucogranite to a typically charnockitic greenish-grey. The charnockitic veins have an unoriented igneous texture that almost, but not entirely, obliterates the gneissic texture of the host rock (Fig. 4F), and there is no evidence of a chilled margin. They comprise randomly oriented subhedral megacrystic plagioclase, perthite, microperthite and aggregates of fine-grained biotite, chlorite, calcite, dolomite and ilmenite which are pseudomorphic after orthopyroxene grains. Relative to the host gneisses, the charnockitic veins are depleted in Fe, Mg, Mn, Ti, Ca, P, Nb, Zr, Y, U, Th, Ta, Sc and HREE,

and enriched in K, Ba, Sb, Pb, Sr, Rb and LREE. Si, Al and Na were immobile (Saunders, 1995; Fig. 13).

The igneous textures of the charnockite veins indicate a super-solidus, i.e. melting, origin, but the lack of evidence for magmatic intrusion (e.g. local preservation of "ghost" foliation within the charnockite that is continuous from the country rock across the contact, see Fig. 4F) suggests that they were produced *in situ*. *In situ* fluid-absent melting of a biotite (hydrous phase) bearing gneiss can be initiated by an increase in temperature (>850 °C) or a decrease in pressure at high temperature through the breakdown of biotite by reaction with quartz to produce an anhydrous phase such as orthopyroxene or garnet which releases water that in turn fluxes a partial melt (Waters and Whales, 1984; Clemens, 1993; Stevens and Clemens, 1993; Vielzeuf and Montel, 1994; Stevens et al., 1997). It is this anatectic process that was proposed for the origin of the concordant syn-D2 garnetiferous and charnockitic leucosomes by Saunders (1995). However, the post-D2 charnockitic veins are not associated with the regional metamorphic event as they are discordant to the regional tectonic fabric, and they do not display any of the typical migmatitc features such as mafic selvages of restitic material as seen in the syn-D2 leucosomes. Instead, their restriction to small sinistral faults favours a fluid-initiated melting process rather than a pervasive temperature increase. Saunders (1995) proposed that charnockitisation was a result of the introduction of partially hydrous (C-O-H) fluids under granulite facies conditions along structural dislocations. The introduction of such fluids would flux localized anatexis adjacent to the discontinuities to produce the pegmatitic charnockite veins. The water would be preferentially partitioned into the melt phase leaving behind a CO_2-rich fluid, thus explaining the abundant CO_2 fluid inclusion within these charnockites. Moreover, the retrograde carbonate

alteration of the orthopyroxene can be ascribed to low temperature reaction with the remnant CO_2-rich fluids. The small sinistral faults were probably produced during post-D2 uplift while the rocks were still hot (granulite facies). The origin of the carbonic (C-O-H) fluids could be related to granulite facies devolatilization of the nearby carbonate supracrustals of the Marble Delta Formation in the Margate Terrane (Fig. 3; Saunders, 1995). Alternatively, adjacent plutons of intruding Oribi Gorge Suite which probably had CO_2 bearing fluids similar to those recorded in the Port Edward Pluton could have provided a source.

5. Conclusions

Exposures in the Mesoproterozoic Natal belt show four main types of charnockite formation and their inter-relationships. It thus constitutes an important area for studies of charnockite genesis on a par with, if not superior to, the classic southern India localities. The descriptions of the four varieties of charnockites from the Natal belt in this article show that orthopyroxene-bearing rocks with igneous textures can originate both from crystallization of dry, high-temperature, mantle-derived, differentiated mafic melts (magmatic charnockites), and by subsolidus metamorphic and metasomatic alteration of granitoid rocks at high temperatures and in the presence of fluids with low water activities (metamorphic charnockites). New C isotope data presented here show that the CO_2-rich fluids associated with magmatic charnockites were mantle-derived. The origins of the metamorphic fluids involved in sub-solidus fluid related charnockitisation are not as well constrained, but field evidence suggests that these may have been introduced by intruding magmas and/or devolatilization of nearby carbonates during metamorphism. However, the distinction between magmatic and metamorphic charnockites can

be blurred as in the example of nebulous charnockitic veins of the Margate Suite Granite which have been interpreted as originating from *in situ*, post-emplacement, localized, fluid-induced melting (super-solidus charnockitisation) during later metamorphism. Moreover, the required low water activities in magmatic fluids need not be an inherent characteristic of the parent magmas but can also arise through interaction with country rock as in the case of the Portobello granite. The unequivocal field relationships and exposures in the Natal belt facilitate the clear distinction between magmatic and subsolidus charnockite genesis. In areas where such unequivocal exposures of orthopyroxene-bearing granitoid are absent, the uncertainty in recognizing whether the rocks are magmatic or metamorphic in origin has implications for the applicable nomenclature of such rocks, in view of a recent suggestion that the term charnockite should be reserved for those rocks clearly of magmatic origin (Frost and Frost, 2008). We do not subscribe to this view.

Acknowledgments

RJT thanks the CEO, NERC BGS for permission to publish. This paper is dedicated to John McIver who made the first detailed study of the charnockites of the Natal South Coast and who sadly passed away while it was being prepared. We would like to acknowledge constructive reviews by Dr. R. Voordouw and Dr. Lopamudra Saha. Samples with the prefix UND from the Port Edward pluton were analyzed from powders supplied to GHG by Bruce Eglington who is gratefully acknowledged.

References

Allen, P., Condie, K.C., Narayana, B.L., 1985. The geochemistry of prograde and retrograde charnockite-gneiss reactions in southern India. Geochimicha et Cosmochimica Acta 49, 323-336.

Aranovich, L.Y., Newton, R.C., 1995. Experimental determination of CO_2-H_2O activity-composition relations at 600–1000 °C and 6–14 kbar by reversed decarbonation and dehydration reactions. American Mineralogist 84, 1319-1332.

Arima, M., Tani, K., Kawate, S., Johnston, S.T., 2001. Geochemical characteristics and tectonic setting of metamorphosed rocks from the Tugela terrane, Natal belt, South Africa. Memoirs of the National Institute of Polar Research Japan, Special Issue 55, 1-39.

Barkhuizen, J.G., Matthews, P.E., 1990. Gravity modelling of the Natal Thrust Front: a Mid-Proterozoic crustal suture in southeastern Africa. Geocongress'90 absracts, University of Cape Town, 32–35.

Bisnath, A., McCourt, S., Frimmel, H.E., Buthelezi, S.B.N., 2008. The metamorphic evolution of mafic rocks in the Tugela Terrane, Natal Belt, South Africa. South African Journal of Geology 111, 369-386.

Bohlender, F., van Reenen, D.D., Barton, J.M., 1992. Evidence for metamorphic charnockites in the southern Marginal Zone of the Limpopo Belt. Precambrian Research 55, 429-449.

Clemens, J.D., 1992. Partial melting and granulite genesis: A partisan overview. Precambrian Research 55, 297-301.

Clemens, J.D., 1993. Experimental evidence against CO_2-promoted deep crustal melting. Nature 363, 336-338.

Cornell, D.H., Thomas, R.J., 2006. Age and tectonic significance of the Banana Beach Gneiss, KwaZulu-Natal south coast, South Africa. South African Journal of Geology 109, 335-340.

Deines, P., 2000. The carbon isotope geochemistry of mantle xenoliths. Earth Science Reviews 58, 247-278.

Du Toit, A.L., 1946. The geology of parts of Pondoland, East Griqualand and Natal. Geological Survey of South Africa, Explanation Sheet 119.

Ebadi, A., Johannes, W., 1991. Beginning of melting and components of first melts in the system Qz-Ab-Or-H_2O-CO_2. Contributions to Mineralogy and Petrology 106, 286-295.

Eglington, B.M., 2006. Evolution of the Namaqua-Natal Belt, southern Africa – A geochronological and isotope geochemical review. Journal of African Earth Sciences 46, 93-111.

Eglington, B.M., Harmer, R.E., Kerr, A., 1986. Petrographic, Rb-Sr isotope and geochemical characteristics of intrusive granitoids from the Port Edward - Port shepstone area, Natal. Transactions of the Geological Society of South Africa 89, 199-213.

Eglington, B.M., Thomas, R.J., Armstrong, R.A., Walraven, F., Kerr, A., Retief, E.A., 2003. Zircon geochronology of the Oribi Gorge Suite, Kwa-Zulu Natal, South Africa: constraints on the timing of transcurrent shearing in the Namaqua-Natal Belt. Precambrian Research 123, 29-46.

Eglington, B.M., Thomas, R.J., Armstrong, R.A., 2010. U-Pb SHRIMP zircon dating of Mesoproterozoic magmatic rocks from the Scottburgh area, central Mzumbe terrane, KwaZulu-Natal, South Africa. South African Journal of Geology 113, 229-235.

Farquhar, J., Chacko, T., 1991. Isotopic evidence for involvement of CO_2-bearing magmas in granulite formation. Nature 354, 60-63.

Friend, C.R.L., 1981. Charnockite and granite formation and influx of CO_2 at Kabbaldurga. Nature 294, 550-553.

Frost, B.R., Frost, C.D., 2008. On charnockites. Gondwana Research 13, 30-44.

Fyfe, W.S., 1973. The granulite facies, partial melting and the Archaean crust. Pholisophical Transactions Royal Society London A273, 457-461.

Gevers, T.W., 1941. Carbon dioxide and exhalations in northern Pondoland and Alfred County, Natal. Transactions of the Geological Society of South Africa 45, 223-301.

Gevers, T.W., Dunne, J.C., 1942. Charnockitic rocks near Port Edward in Alfred County, Natal. Transactions of the Geological Society of South Africa 45, 183-214.

Grantham, G.H., 1984. The tectonic, metamorphic and intrusive history of the Natal Mobile Belt between Glenmore and Port Edward, Natal. M.S. thesis, University of Natal (Pietermaritzburg), 243pp.

Grantham, G.H., Allen, A.R., Cornell, D.H., Harris, C., 1996. Geology of Nicholson's point granite, Natal Metamorphic Province, South Africa: the chemistry of charnockitic alteration and origin of the granite. Journal of African Earth Sciences 23, 465-484.

Grantham, G.H., Eglington, B.M., Thomas, R.J., Mendonidis, P., 2001. The nature of the Grenville-age Charnockitic A-type magmatism from the Natal, Namaqua and Maud Belts of southern Africa and western Dronning Maud Land, Antarctica. National Institute of Polar Research, Tokyo, Special Issue 55, 59-86.

Green, T.H., Pearson, N.J., 1986. Ti-rich accessory phase saturation in hydrous mafic-felsic compositions at high P, T. Chemical Geology 54, 185-201.

Hansen, E.C., Janardhan, A.S., Newton, R.C., 1984. Fluid inclusions in rocks from the amphibolite-facies to charnockite progression in southern Karntaka, India: Direct evidence concerning the fluids of granulite metamorphism. Journal of Metamorphic Geology 2, 249-264.

Hansen, E.C., Janardhan, A.S., Newton R.C., Prame, W.K.B.N., Ravindra, G.R., 1987. Arrested charnockite formation in southern India and Sri Lanka. Contributions to Mineralogy and Petrology 96, 225-244.

Hansen, E.C., Newton R.C., Janardhan, A.S., Lindebburg, S., 1995. Differentiation of late Archaean crust in the eastern Dharwar Craton, Krishnagiri-Salem Area, south India. Journal of Geology 103, 629-651.

Harrison, T.M., Watson, E.B., 1984. The behavior of apatite during crustal anatexis: Equilibrium and kinetic considerations. Geochimica et Cosmochimica Acta 48, 1467-1477.

Holland, T.J.B., Powell, R., 1998. An internally consistent thermodynamic dataset for phases of petrological interest. Journal of Metamorphic Geology 16, 309-343.

Huizenga, J.M., Touret, J.L.R., 2012. Granulites, CO_2 and graphite. Gondwana Research, http://dx.doi.org/10.1016/j.gr.2012.03.007.

Irvine, T.N., Barager, W.R.A., 1971. A guide to the chemical classification of the common volcanic rocks. Canadian Journal of Earth Science 8, 523-548.

Jackson, D.H., Mattey, D.P., Harris, N.B.W., 1988. Carbon isotope compositions of fluid inclusions in charnockites from southern India. Nature 333, 167-170.

Jacobs, J., Thomas, R.J., Weber, K., 1993. Accretion and indentation tectonics at the southern edge of the Kaapvaal craton during the Kibaran (Grenville) orogeny. Geology 21, 203-206.

Janardhan, A.S., Newton, R.C., Smith, J.V., 1979. Ancient crustal metamorphism at low pH_2O and charnockite formation at Kabbaldurga, South India. Nature 278, 511-514.

Janardhan, A.S., Newton, R.C., Hansen, E.C., 1982. The transformation of amphibolite facies gneiss to charnockite in southern Karnataka and northern Tamil Nadu, India. Contributions to Mineralogy and Petrology 79, 130–149.

Johnston, S.T., Armstrong, R.A., Heaman, L., McCourt, S., Mitchell, A., Bisnath, A., Arima, M., 2001. Preliminary U-Pb geochronology of the Tugela Terrane, Natal Belt, eastern South Africa. Memoir National Institute of Polar Research, Special Issue 55, 40-58.

Johnston, S.T., McCourt, S., Bisnath, A., Mitchell, A.A., 2003. The Tugela Terrane, Natal Belt: Kibaran magmatism and tectonism along the south eastern margin of the Kaapvaal Craton. South African Journal of Geology 106, 85-97.

Kerr, A., 1985. Characterization of the granitic rocks from the Valley of a Thousand Hills area, Natal. South African Journal of Science 81, 475-478.

Kilpatrick, J.A., Ellis, D.J., 1992. C-type magmas: Igneous charnockites and their extrusive equivalents. Transactions Royal Society Edinburgh: Earth Sciences 83, 155-164.

Kretz, R., 1983. Symbols for rock-forming minerals. American Mineralogist 68, 277-279.

Kumar, G.R.R., 2004. Mechanism of arrested charnockite formation at Nemmara, Palghat region, southern India. Lithos 75, 331-358.

Le Maitre, R.W., 2002. Igneous Rocks: A Classification and Glossary of Terms. Cambridge University Press, New York, 236.

Lindsley, D.H., 1983. Pyroxene thermometry. American Mineralogist 68, 477-493.

Luque, F.J., Crespo-Feo, E., Barrenechea, J.G., Ortega, L., 2012. Carbon isotopes of graphite: Implications on fluid history. Geoscience Frontiers 3, 197-207.

Martignole, J., 1979. Charnockite genesis and the Proterozoic crust. Precambrian Research 9, 303-310.

Matthews, P.E., 1972. Possible pre-Cambrian obduction and plate tectonics in southeastern Africa. Nature 240, 37-39.

Mattey, D.P., 1991. Carbon dioxide solubility and carbon isotope fractionation in basaltic melt. Geochimica et Cosmochimica Acta 55, 3467-3473.

McCourt, S., Armstrong, R.A., Grantham, G.H., Thomas, R.J., 2006. Geology and evolution of the Natal Belt, South Africa. Journal of African Earth Sciences 46, 71-92.

McIver, J.R., 1963. A contribution to the Precambrian geology of southern Natal. PhD thesis, University of Witwatersrand, 203pp.

McIver, J.R., 1966. Orthopyroxene-bearing granitic rocks from southern Natal. Transactions of the Geological Society of South Africa 66, 99-117.

Mendonidis, P., Armstrong, R.A., Grantham, G.H., 2009. U-Pb SHRIMP ages and tectonic setting of the Munster Suite of the Margate Terrane of the Natal Metamorphic Belt. Gondwana Research, 15, 28-37.

Mendonidis, P., 1989. The tectonic evolution of a portion of the Southern Granulite Zone of the Natal Mobile Belt, between Southbroom and Glenmore, Natal. PhD thesis, University of Natal, Pietermaritzburg, 260 pp.

Mendonidis, P., Armstrong, R.A., Eglington, B.M., Grantham, G.H., Thomas, R.J., 2002. Metamorphic history and U-Pb zircon (SHRIMP) geochronology of the Glenmore Granite: implications for the tectonic evolution of the Natal Metamorphic Complex. South African Journal of Geology 105, 325-336.

Mendonidis, P., Armstrong, R.A., 2009. A new U-Pb zircon age for the Portobello granite from the southern part of the Natal Metamorphic Belt. South African Journal of Geology, 112, 197-208.

Mendonidis, P., Grantham, G.H., 2003. Petrology, origin and Metamorphic History of Proterozoic-aged Granulites of the Natal Metamorphic province, southeastern Africa. Gondwana Research 6, 607-628.

Mendonidis, P., Grantham, G.H., 1989. The distribution, petrology and geochemistry of the Munster Suite, south coast, Natal. South African Journal of Geology 92, 377-388.

Mendonidis, P., Grantham, G.H., 1990. Munster Suite. In: Catalogue of South African Lithostratigraphic Units 2, 33-34.

Mendonidis, P., Grantham, G.H., 2005. Geochemistry of the charnockitic marginal phase of the portobello granite, natal metamorphic province. GEO2005 Conference Abstracts, Geological Society of South Africa, Durban, p154-155.

Mendonidis, P., Grantham, G.H., 2000. Rare earth element distribution and modelling in charnockitic aureoles from southern Natal. Journal of African Earth Sciences 31, 51.

Mendonidis, P., Strydom, D., 1989. Tectonic history of Proterozoic granulite gneisses between Glenmore and Southbroom, southern Natal. South African Journal of Geology 92, 352-368.

Mendonidis, P., Grantham, G.H., Thomas, R.J., 1991. Glenmore Granite. In: Johnson, M.R. (Ed.), Catalogue of South African Lithostratigraphic Units, South African Committee for Stratigraphy, 13-14.

Miller, M.F., Pillinger, C.T., 1997. An appraisal of stepped heating release of fluid inclusion CO_2 for isotopic analysis: A preliminary to $\delta^{13}C$ characterization of carbonaceous vesicles at the nanomole level. Geochimica et Cosmochimica Acta 61, 193-205.

Naney, M.T., 1983. Phase equilibria of rock-forming ferromagnesian silicates in granitic systems. American Journal of Science 283, 993-1033.

Naney, M.T., Swanson, S.E., 1980. The effects of Fe and Mg on crystallisation in granitic systems. American Mineralogist 65, 639-653.

Newton, R.C., Smith, J.V., Windley, B.F., 1980. Carbonic metamorphism, granulites and crustal growth. Nature 288, 45-50.

Newton, R.C., Hanson, E.C., 1983. The origin of Proterozoic and late Archaean charnockites—evidence from field relations and experimental petrology. In: Medaris, L.G., et al. (Eds.), Proterozoic geology. Geological Society of America Memoir 161, p167-178.

Papineau, D., De Gregorio, B.T., Cody, G.D., Fries, M.D., Mojzsis, S.J., Steele, A., Stroud, R.M., Fogel, M.L., 2010. Ancient graphite in the Eoarchean quartz-pyroxene rocks from Akilia in southern West Greenland I: Petrographic and spectroscopic characterization. Geochimica et Cosmochimica Acta 74, 5862-5883.

Purchuk, L.L., Gerya, T.V., 1993. Fluid control of charnockitsation. Chemical Geology 108, 175-186.

Raith, M., Srikantappa, C., 2007. Arrested charnockite formation at Kottavattam, southern India. Journal of Metamorphic Petrology 1196, 815-832.

Santosh, M., Jackson, D.H., Harris, N.B.W., Mattey, D.P., 1991. Carbonic fluid inclusions in South Indian granulites: evidence for entrapment during charnockite formation. Contributions to Mineralogy and Petrology 108, 318-330.

Santosh, M., Omori, S., 2008. CO_2 windows from mantle to atmosphere: models on ultra-high temperature metamorphism and specifications on the link with melting of snowball Earth. Gondwana Research 14, 82–96.

Satish-Kumar, M., 2005. Graphite-bearing CO_2-fluid inclusions in granulites: Insights on graphite precipitation and carbon isotope evolution. Geochimica et Cosmochimica Acta 69, 3841-3856.

Saunders, B., 1995. Fluid-induced charnockite formation post-dating prograde granulite facies anatexis in southern Natal Metamorphic Province, South Africa. M.S. thesis, Rand Afrikaans University, 176 pp.

Saxena, S.K., 1977. The charnockite geotherm. Science 198, 614-617.

Stern, R.J., Dawoud, A.S., 1991. Late Precambrian (740 Ma) charnockite, enderbite, and granite from Jebel Moya, Sudan: A link between the Mozambique Belt and the Arabian-Nubian Shield? Journal of Geology 99, 648-659.

Stevens, G., Clemens, J.D., 1993. Fluid-absent melting and the role of fluids in the lithosphere: a slanted summary? Chemical Geology 108, 1-17.

Stevens, G., Clemens, J.D., Droop, G.T.R., 1997. Melt production during granulite facies anatexis: experimental data from “primitive” metasedimentary protoliths. Contributions to Mineralogy and Petrology 128, 352-370.

Talbot, C.J., Grantham, G.H., 1987. The Proterozoic intrusion and deformation of deep crustal ‘sills’ along the south coast of Natal. South African Journal of Geology 90, 520-538.

Thomas, R.J., 1988a. The geology of the Port Shepstone area. Explanation of sheet 3030 Port Shepstone. Geological Survey of South Africa, Pretoria, 136pp.

Thomas, R.J., 1988b. The petrology of the Oribi Gorge Suite: Kibaran granitoids from southern Natal. South African Journal of Geology 91, 275-291.

Thomas, R.J., 1989. A tale of two tectonic terranes. South African Journal of Geology 92, 306-321.

Thomas, R.J., Mawson, S.A., 1989. Newly discovered outcrops of Proterozoic basement rocks in northeastern Transkei. South African Journal of Geology 92, 369-376.

Thomas, R.J., Eglington, B.M., 1990. A Rb-Sr, Sm-Nd and U-Pb zircon isotopic study of the Mzumbe suite, the oldest intrusive granitoid in southern Natal, South Africa. South African Journal of Geology 93, 761-765.

Thomas, R.J., Mendonidis, P., Grantham, G.H., 1991. Margate Granite Suite. In: Catalogue of South African Lithostratigraphic Units 3, 33-36.

Thomas, R.J., 1991. Oribi Gorge Granitoid Suite. In: Johnson, M.R. (Ed.), Catalogue of South African lithostratigraphic units. South African Committee for Stratigraphy 3, 37-40.

Thomas, R.J., Ashwal, L., Andreoli, M.A.G., 1992. The Turtle Bay Suite: a mafic-felsic granulite association from southern Natal, South Africa. Journal of African Earth Sciences 15(2), 187-206.

Thomas, R.J., Eglington, B.M., Bowring, S.A., Retief, E.A., Walraven, F., 1993a. New isotope data from a Neoproterozoic porphyritic granitoid-charnockite suite from Natal, South Africa. Precambrian Research 62, 83-101.

Thomas, R.J., Eglington, B.M., Bowring, S.A., 1993b. Dating the cessation of Kibaran magmatism in Natal, South Africa. Journal of African Earth Sciences 16, 247-252.

Thomas, R.J., Agenbacht, A.L.D., Cornell, D.H., Moore, J.M., 1994. The Kibaran of southern Africa: Tectonic evolution and metallogeny. Ore Geology Reviews 9, 131-160.

Thomas, R.J., Cornell, D.H., Armstrong, R.A., 1999. Provenance age and metamorphic history of the Quha Formation, Natal Metamorphic Province: a U-Th-Pb zircon SHRIMP study. South African Journal of Geology 102, 83-88.

Thomas, R.J., Armstrong, R.A., Eglington, B.M., 2003. Geochronology of the Sikombe Granite, Transkei, Natal Metamorphic Province, South Africa. South African Journal of Geology 106, 403-408.

Touret, J.L.R., Huizenga, J.M., 2012. Fluid-assisted granulite metamorphism: A continental journey. Gondwana Research 21, 224-235.

Van der Kerkhof, A.M., Grantham, G.H., 1999. Metamorphic charnockite in contact aureoles around intrusive enderbite from Natal. Contributions to Mineralogy and Petrology 137, 115-132.

Van den Kerkhof, A.M., Touret, J.L.R., Maijer, C., Jensen, J.B.H., 1991. Retrograde methane dominated fluid inclusions from high-temperature granulites of Rogaland, southwestern Norway. Geochimica et Cosmochimica Acta 55, 2533-2544.

Vielzuef, D., Montel, J.M., 1994. Partial melting of metagreywackes. Part 1. Fluid absent experiments and phase relationships. Contributions to Mineralogy and Petrology 117, 375-393.

Waters, D.J., Whales, C.J., 1984. Dehydration melting and the granulites transition in metapelites from southern Namaqualand, S. Africa. Contributions to Mineralogy and Petrology 88, 269-275.

Watson, E.B., 1979. Zircon saturation in felsic liquids: Experimental results and applications to trace element chemistry. Contributions to Mineralogy and Petrology 70, 407-419.

Watson, E.B., Capobiano, C.J., 1981. Phosphorous and the rare earth elements in felsic magmas: an assessment of the role of apatite. Geochemica et Cosmochemica Acta 45, 2349-2358.

Watson, E.B., Harrison, T.M., 1983. Zircon saturation revisited: temperature and composition effects in a variety of crustal magma types. Earth and Planetary Science Letters 64, 295-304.

Wentlandt, R.F., 1981. Influence of CO_2 on melting of model granulite facies assemblages: A model for the genesis of charnockites. American Mineralogist 66, 1164-1174.

Whitney, J.A., 1975. The effects of pressure and X_{H_2O} on phase assemblages in four synthetic rock compositions. Journal of Geology 83, 1-32.

Wickham, S.M., 1988. Evolution of the lower crust. Nature 333, 119-120.

Wyllie, P.J., Huang, W., Stern, C.R., Maaloe, S., 1976. Granitic magmas: possible and impossible sources, water contents and crystallization sequences. Canadian Journal Earth Science 13, 1007-1019.

Figure Captions

Figure 1 Locality map of southern Natal Metamorphic Province showing other locality maps and distribution of the Oribi Gorge Suite.

Figure 2 Graphical tabulation of the Natal Metamorphic belt lithologies for which there are published emplacement ages, sorted according to the age scale on the left (After Mendonidis and Armstrong, 2009). Superscripts refer to the source of the age as follows: [1] Johnston et al., 2001; [2] Thomas et al., 1999; [3] Thomas and Eglington, 1990; [4] Eglington et al., 2010; [5] Eglington et al., 2003; [6] Mendonidis et al., 2002; [7] Mendonidis et al., 2009; [8] Mendonidis and Armstrong, 2009; [9] Cornell and Thomas, 2006; [10] Thomas et al., 1993; [11] Thomas et al., 2003; The Sikombe Granite occurs to the south of the Margate Terrane and may or may not be part of a separate block (Thomas et al., 2003). The shaded blocks indicate lithologies that contain charnockitic rocks.

Figure 3 Locality map of Margate Terrane showing the distribution of Munster Suite and other charnockite varieties including the Oribi Gorge Suite and the Margate Granite thermal aureoles and fluid gradient charnockites. Also shown are the locations of detailed maps shown in Figs. 7 and 10. Note also the location of Marble Delta as well as the quarry location where fluid-driven charnockites are exposed.

Figure 4 Photos of various charnockite localities from Natal. (A) The contact zone between the Oribi Gorge Suite (OGS) (Port Edward pluton) and Margate Suite (Nicholson's Point granite, NPG) at Nicholson's Point showing the megacrystic OGS at left. The first 30–40 cm of NPG from the contact is opx-bearing whereas the rest of the NPG has garnet and biotite; (B) Thin section micrograph in plane polarised light of the OGS showing porphyritic plagioclase rimmed by intercumulate quartz, ilmenite and poikilitic pyroxene containing inclusions of apatite and zircon. The field of view is 10 mm; (C) Rapakivi texture in the OGS; (D) Photograph of the contact zone between the Munster Suite (at left), the marginal orthopyroxene zone and the pink Portobello granite at Palm Beach; (E) Charnockitic aureole developed adjacent to a pegmatitic quartz vein intruding the Nicholsons Point granite (Margate Suite) at Nicholsons Point; (F)

Charnockite vein (right) in the garnet biotite bearing Margate Suite at left. The pegmatitic vein intruding the Margate Suite is traceable through the charnockite vein indicating the metamorphic origin of the charnockite. The dark coarse crystals in the charnockite zone are porphyroblastic orthopyroxene.

Figure 5 (A) AFM diagram after Irvine and Barager (1971) showing the difference in Fe/(Fe+Mg) between the Munster Suite (MS) and the Oribi Gorge Suite (PE); (B) Saturation surface thermometry using the Zr and P_2O_5 contents of the Port Edward pluton of the Oribi Gorge Suite (PE) and the Munster Suite (MS); (C) Comparison of the TiO_2 contents of the Port Edward pluton of the Oribi Gorge Suite (PE) and the Munster Suite (MS) with saturation curves at various temperatures after Green and Pearson (1986).

Figure 6 Interpreted crystallization sequence for the Port Edward pluton of the Oribi Gorge Suite and the Munster Suite, modified after Naney (1983) and Naney and Swanson (1980).

Figure 7 Detailed geological map of the charnockitic zones adjacent to the Munster Suite at Palm Beach. Note the development of the charnockitic Margate Suite adjacent to the quartz monzonoritic Munster Suite.

Figure 8 Thin section photographs from the Portobello granite (A, B, C and D) and the Nicholsons's Point granite. Field of view is ~3 mm with plane polarised light images at left and crossed polar images at right. A–B: Photomicrographs from the chlorite bearing Portobello granite. Note also the more altered feldspars; C–D: Photomicrographs from the charnockitic Portobello granite; E–F: Photomicrographs from the garnet+biotite bearing Nicholsons Point granite. Note the inclusion free subhedral garnet iferred to be of igneous origin; G–H: Photomicrographs from the charnockitic Nicholsons's Point granite.

Figure 9 Plot of whole rock chemistry of charnockitic marginal zones of the Portobello granite normalized against the host biotite chlorite granite. Data from Mendonidis and Grantham (unpublished). The marked depletion in yttrium and niobium is probably because the distribution and migration of these elements is largely controlled by accessory phosphate phases that are

relatively insoluble in felsic liquids. Clear enrichment in Ca, Ba and Sr is evident in the charnockitic Portobello granite, which is probably due to assimilation of country rock plagioclase.

Figure 10 T-X_{H_2O} diagram for the wet granite solidus after Ebadi and Johannes (1991) and two dehydration reaction curves for quartz plus annite (Fe) and phlogopite (Mg) to form orthopyroxene and K feldspar (in the melt) at 5 kb. The reaction curves were calculated using THERMOCALC (Holland and Powell, 1998). The horizontal arrows show the effect of a decreasing fluid gradient inferred to have assisted the crystallization of orthopyroxene in the contact zone applicable to the Portobello Granite at Palm Beach. The vertical double-headed arrow shows the thermal dessication effect of heating by adjacent intrusions resulting in contact metamorphic charnockitic aureoles as seen at Nicholson's Point.

Figure 11 Geological map of Nicholson's Point showing the development of charnockite in aureoles adjacent to Port Edward enderbite of the Oribi Gorge Suite as well adjacent to thin pegmatite veins.

Figure 12 Plot of whole rock chemistry of charnockitic aureoles normalized against the mean of the garnet biotite granite from Nicholson's Point Granite at Nicholson's Point. Data from Grantham et al. (1996).

Figure 13 Plot of whole rock chemistry of post-D2 charnockitic veins normalized against the immediate host rocks, from the Mzimkulu and Beacon Lot quarries. Data from Saunders (1995).

Figure 1

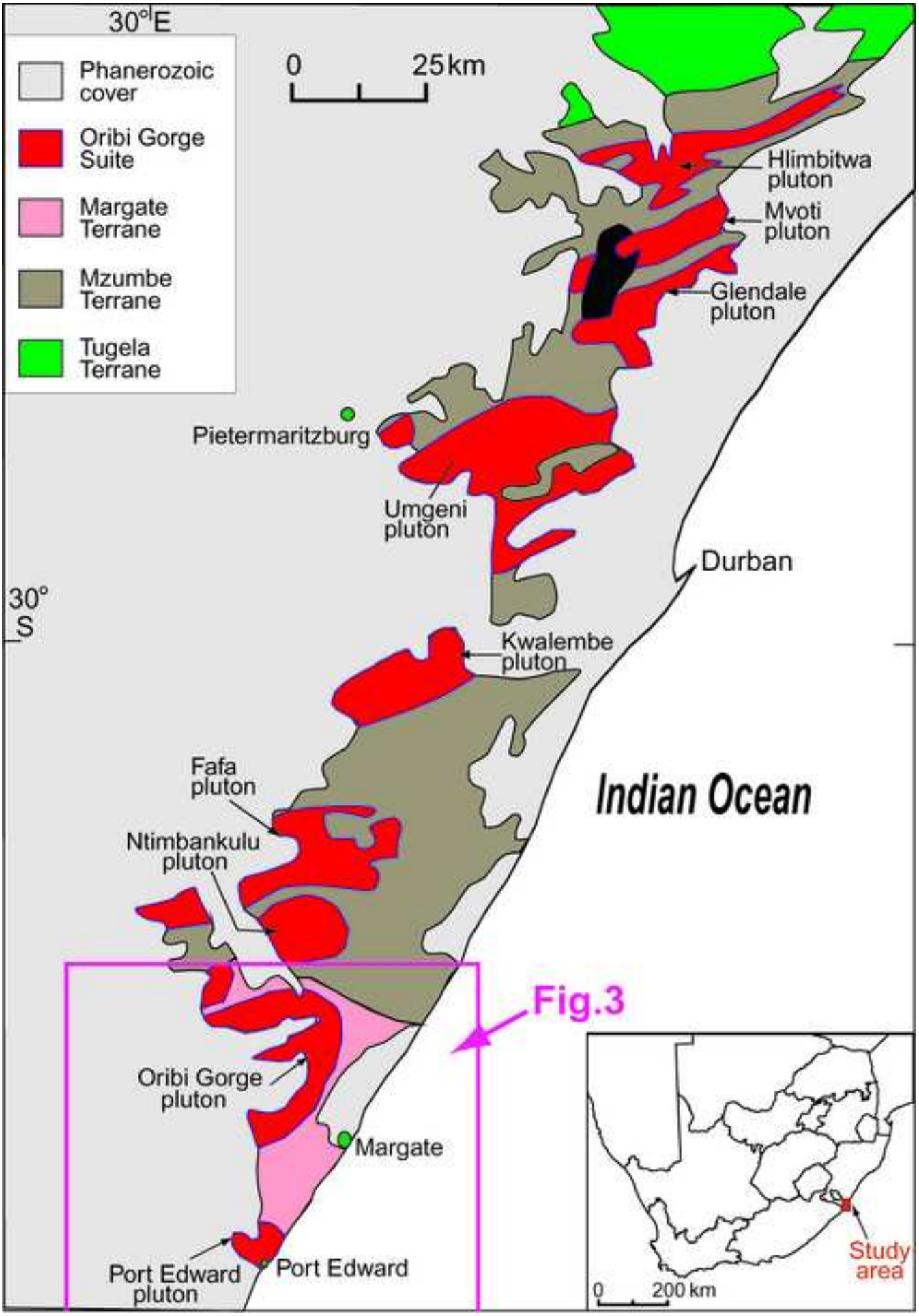

Figure 2

Click here to download high resolution image

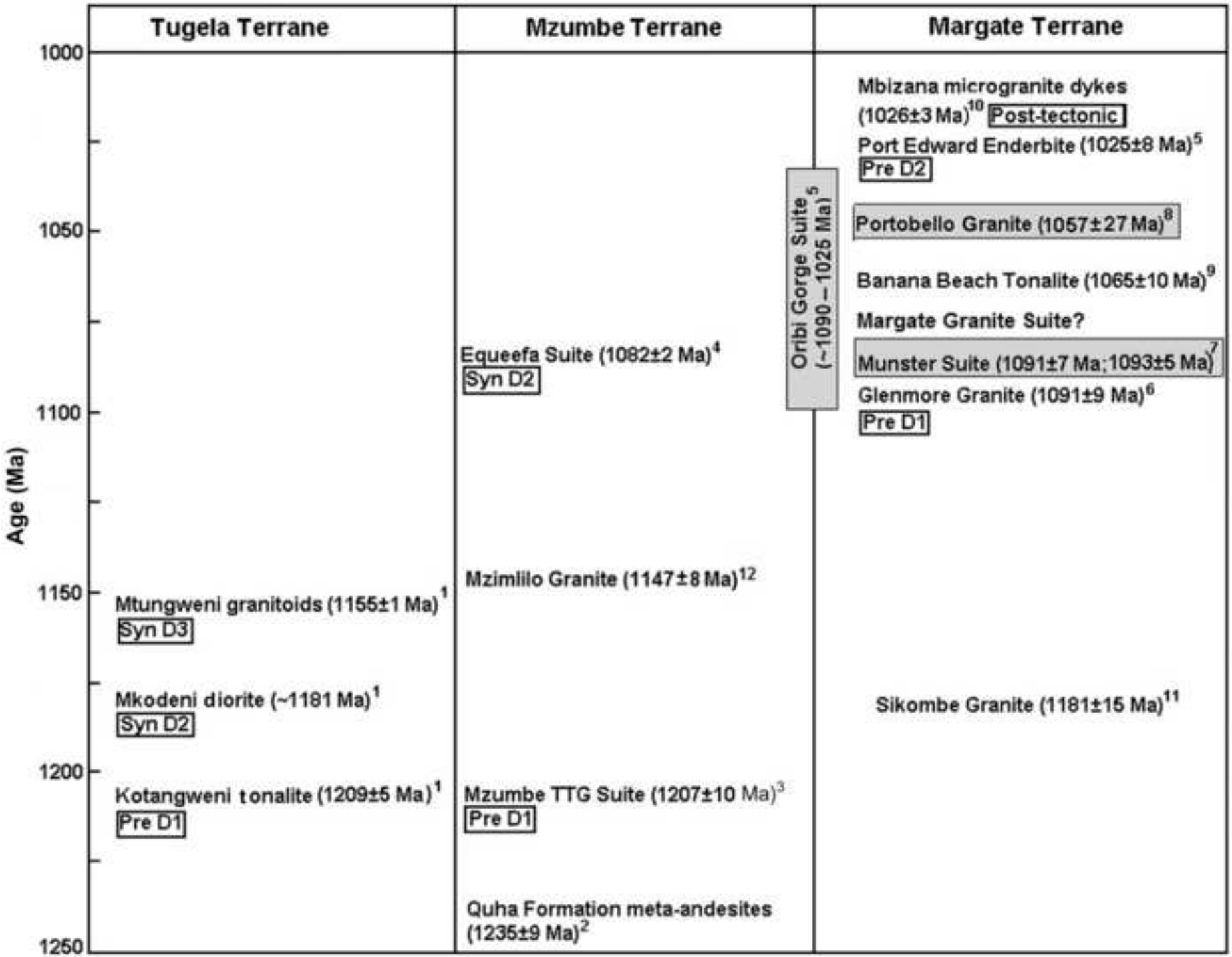

Figure 3

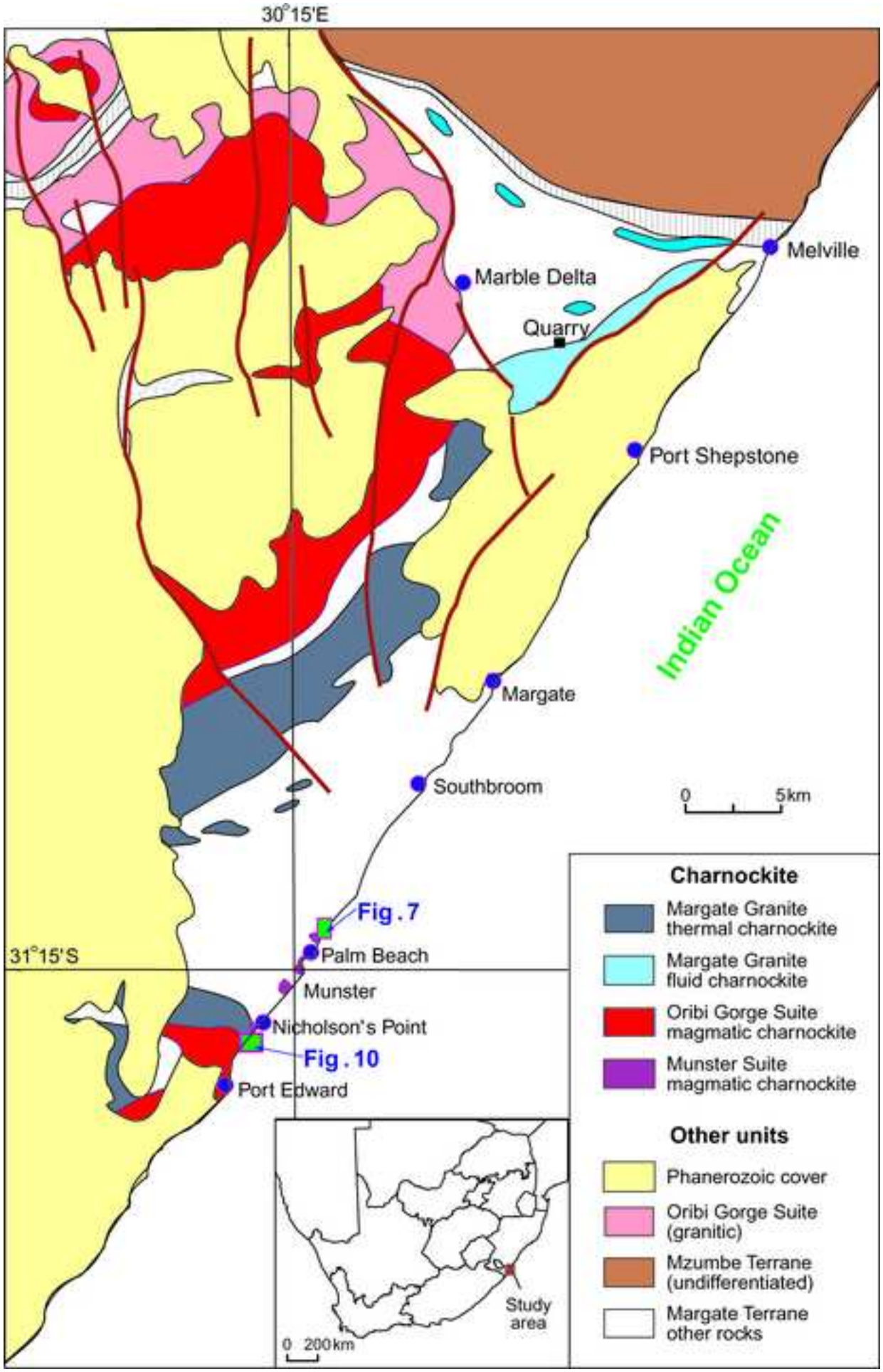

Figure 4

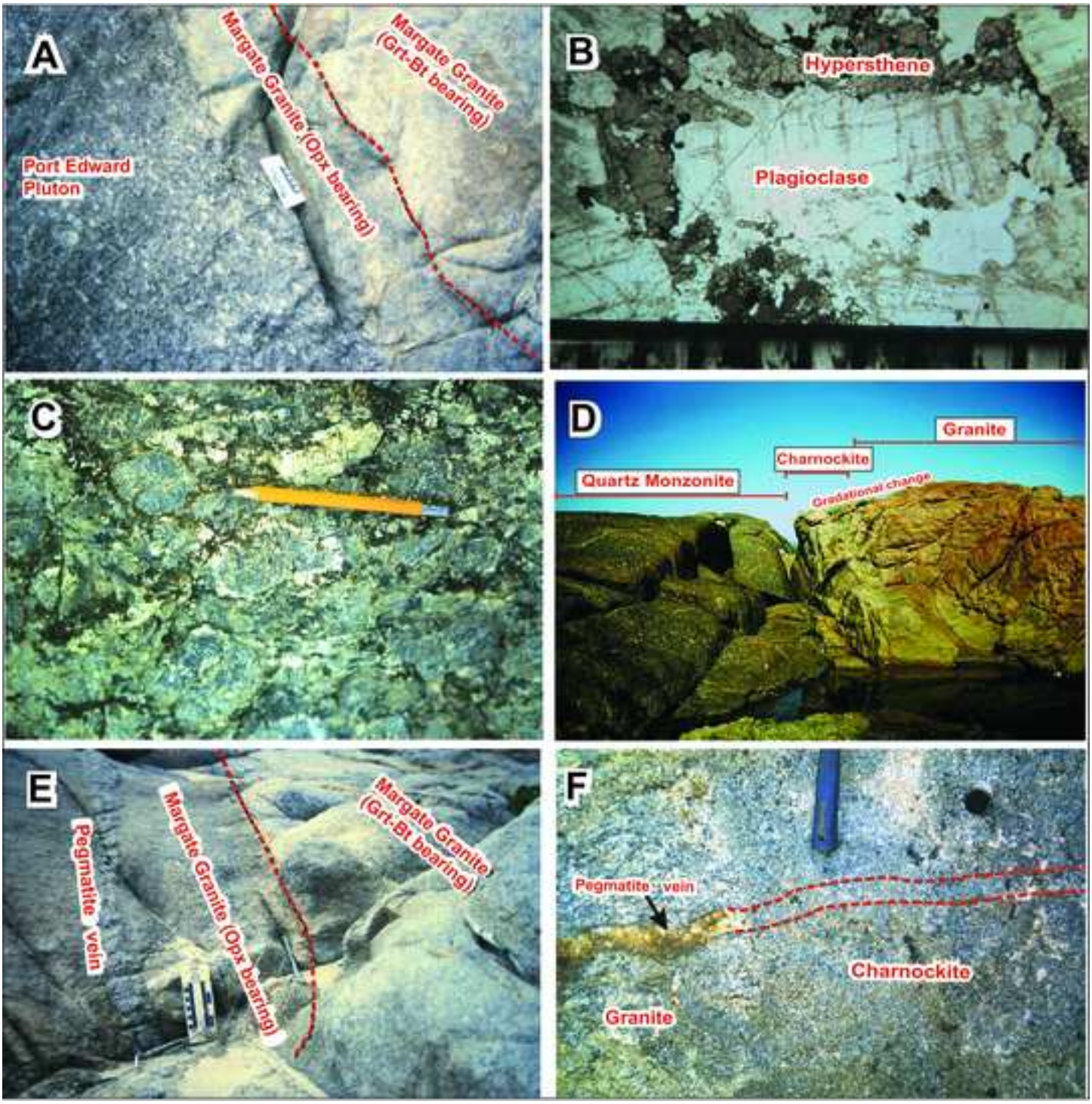

Figure 5

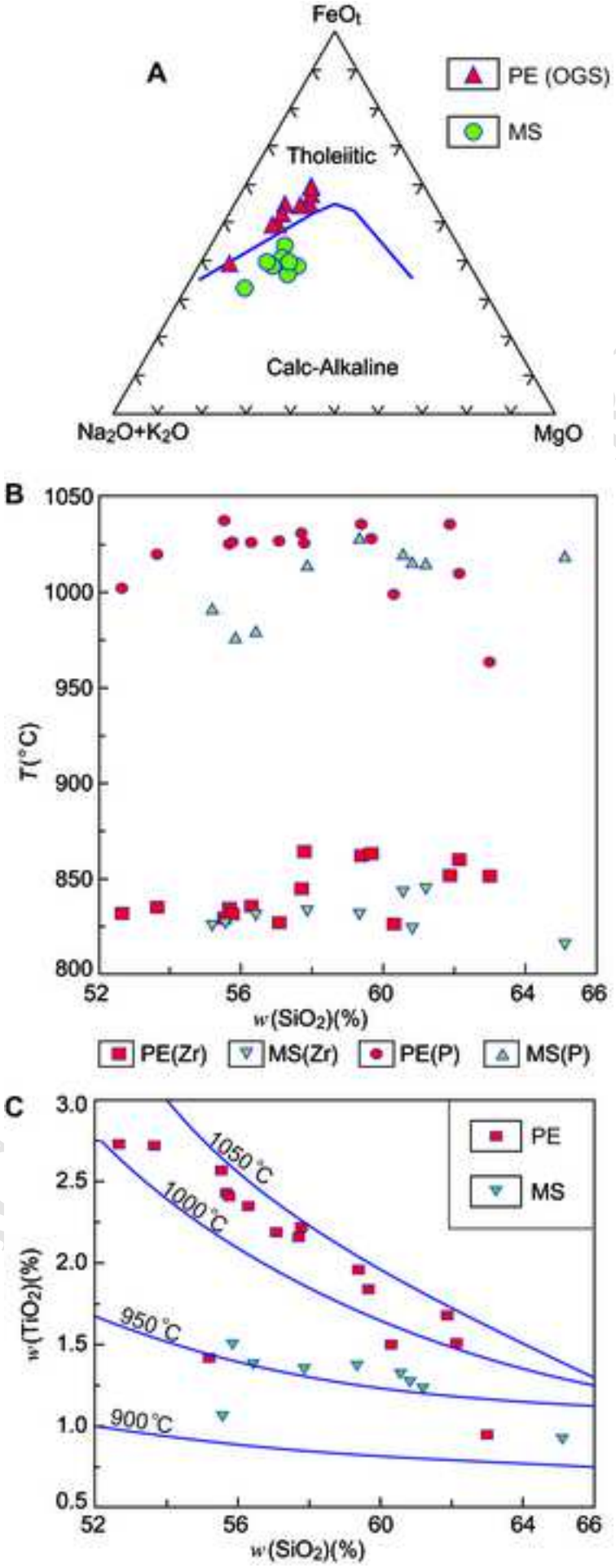

Figure 6

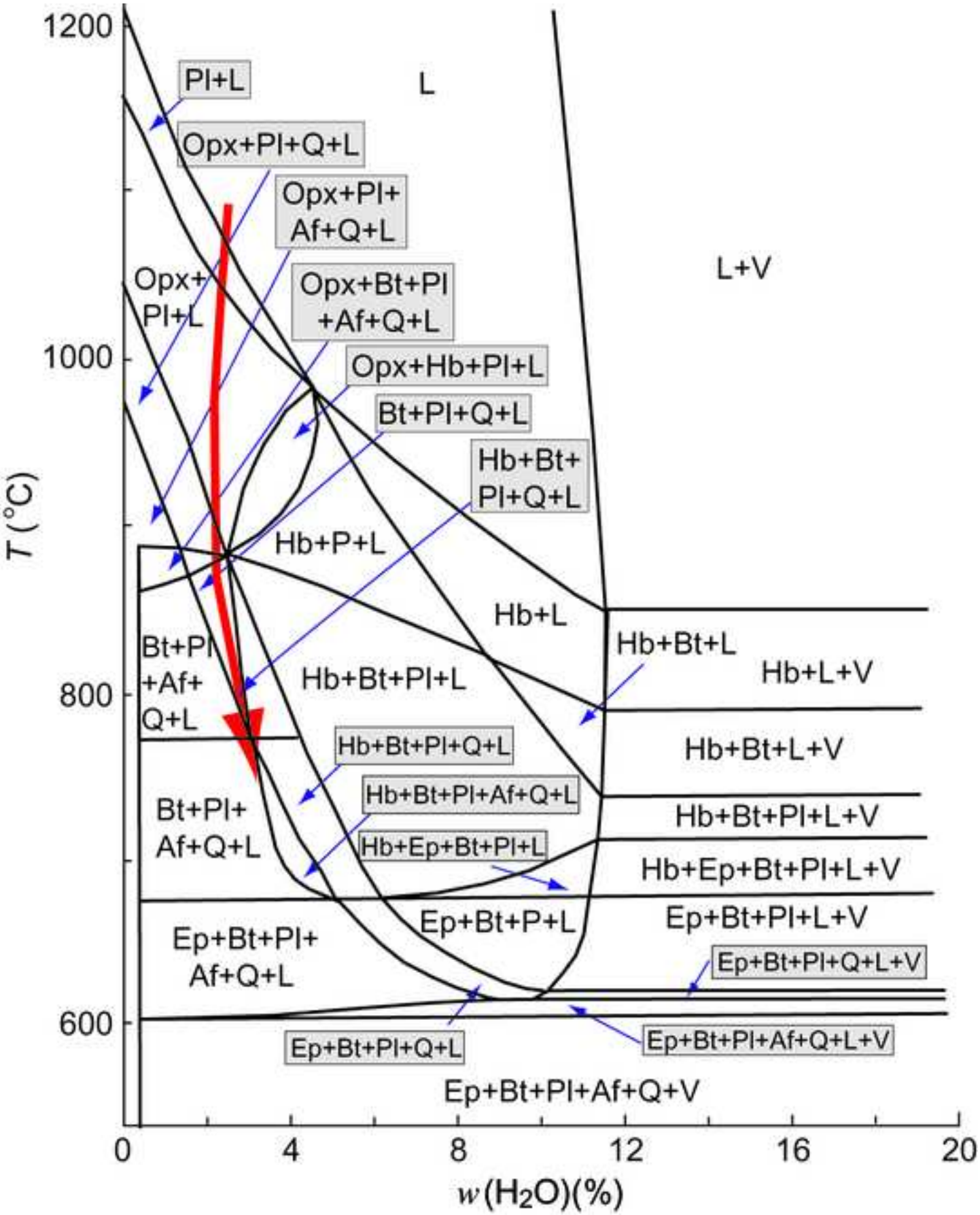

Figure 7

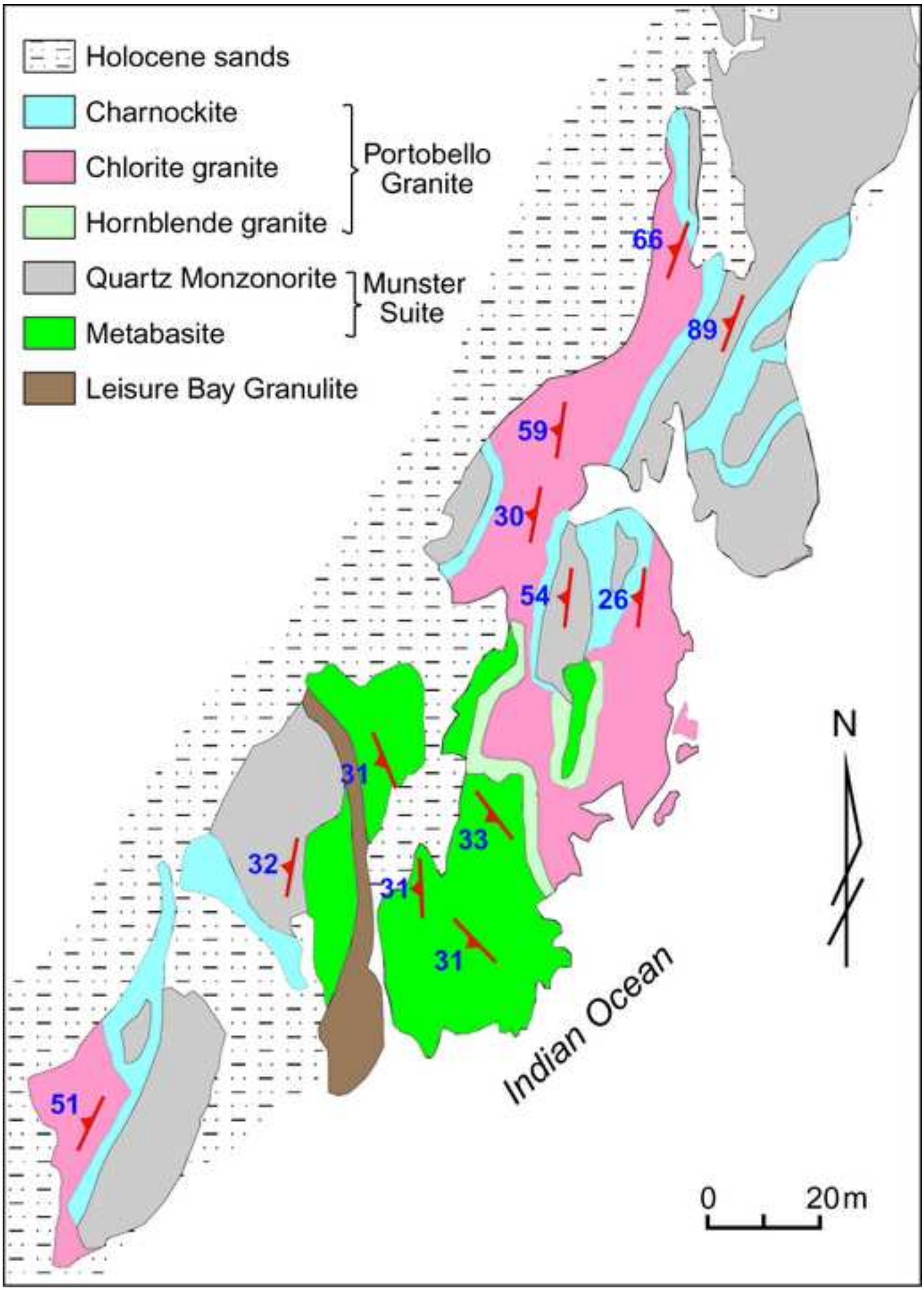

Figure 8

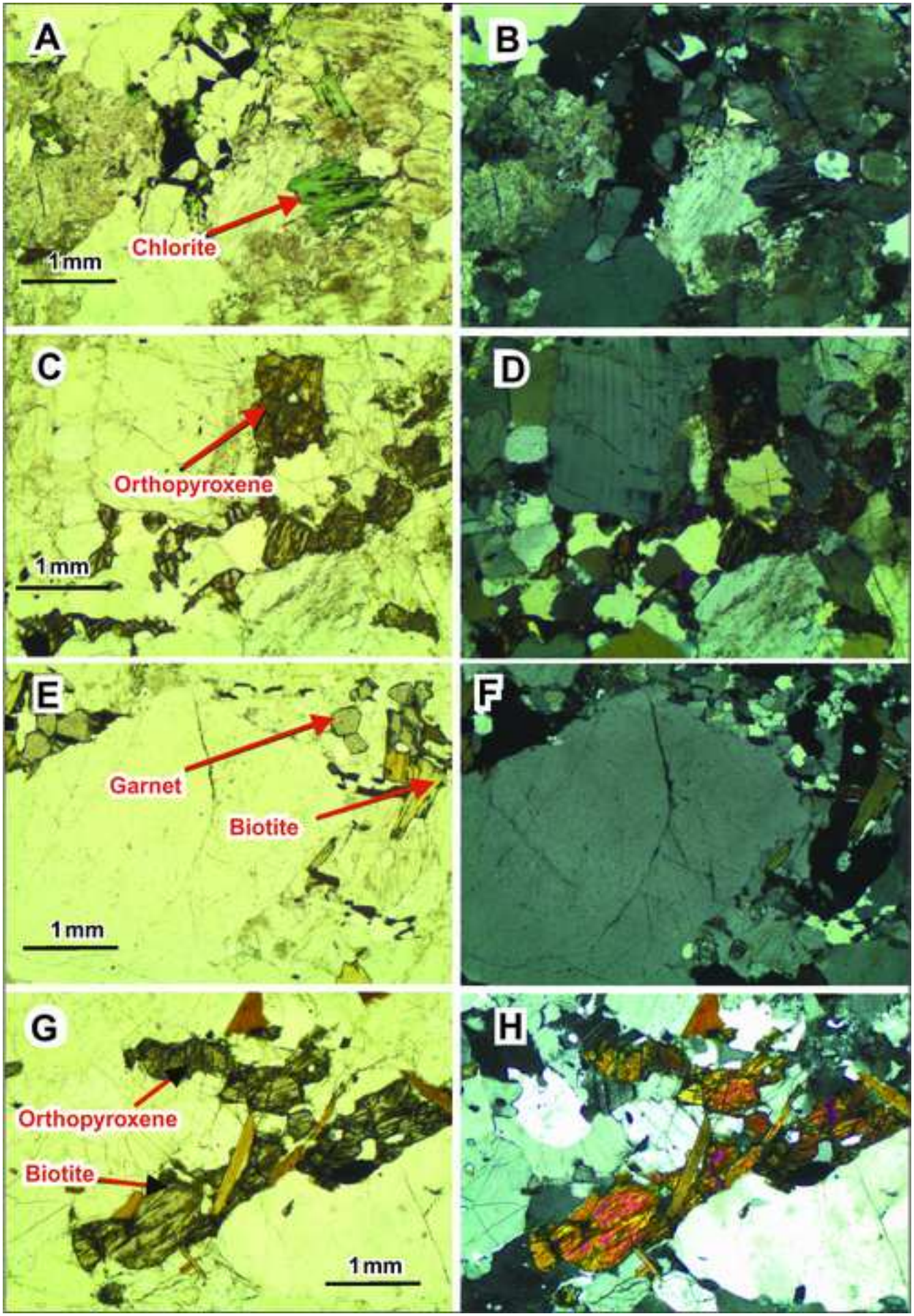

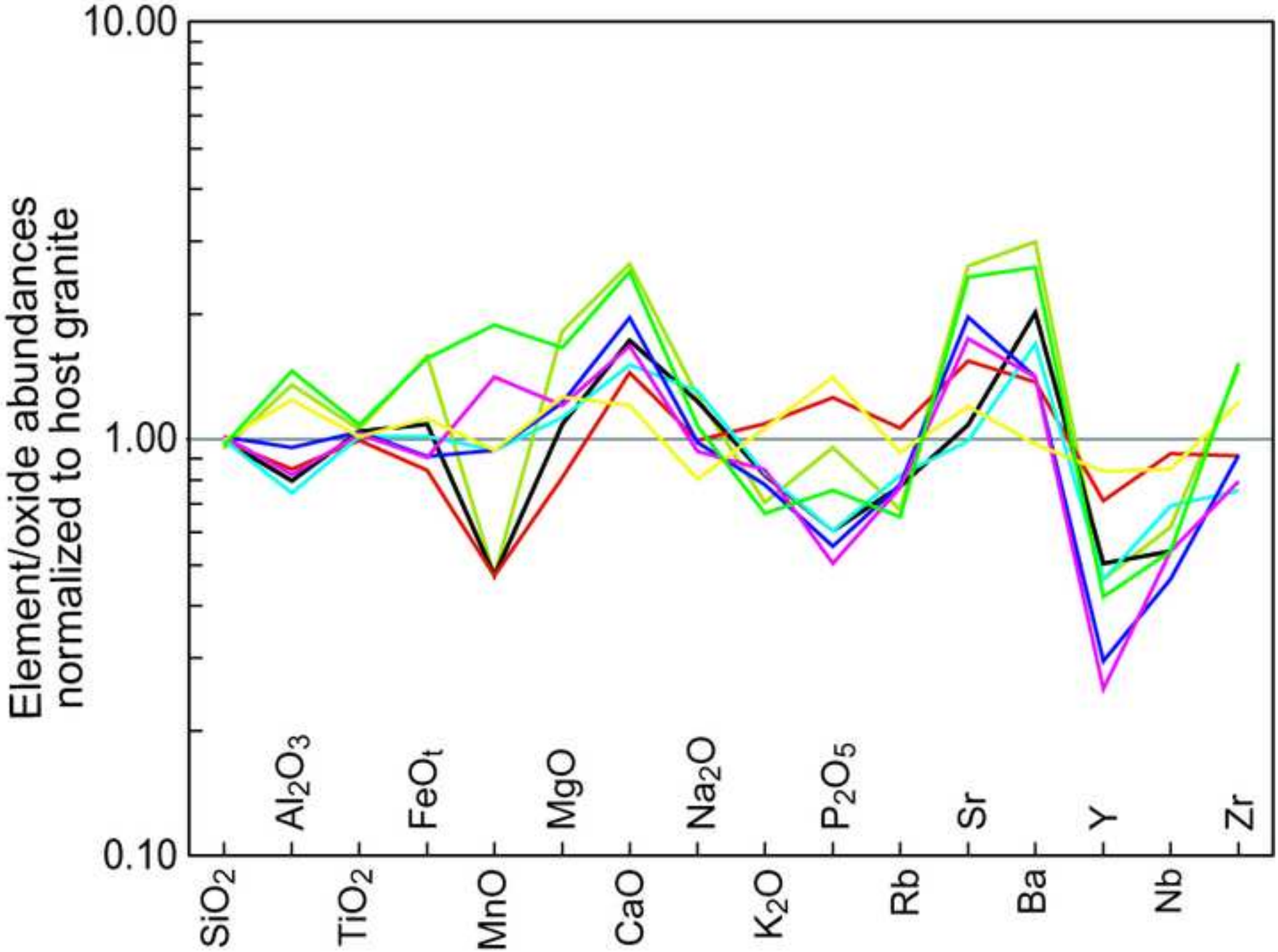

Figure 10

Click here to download high resolution image

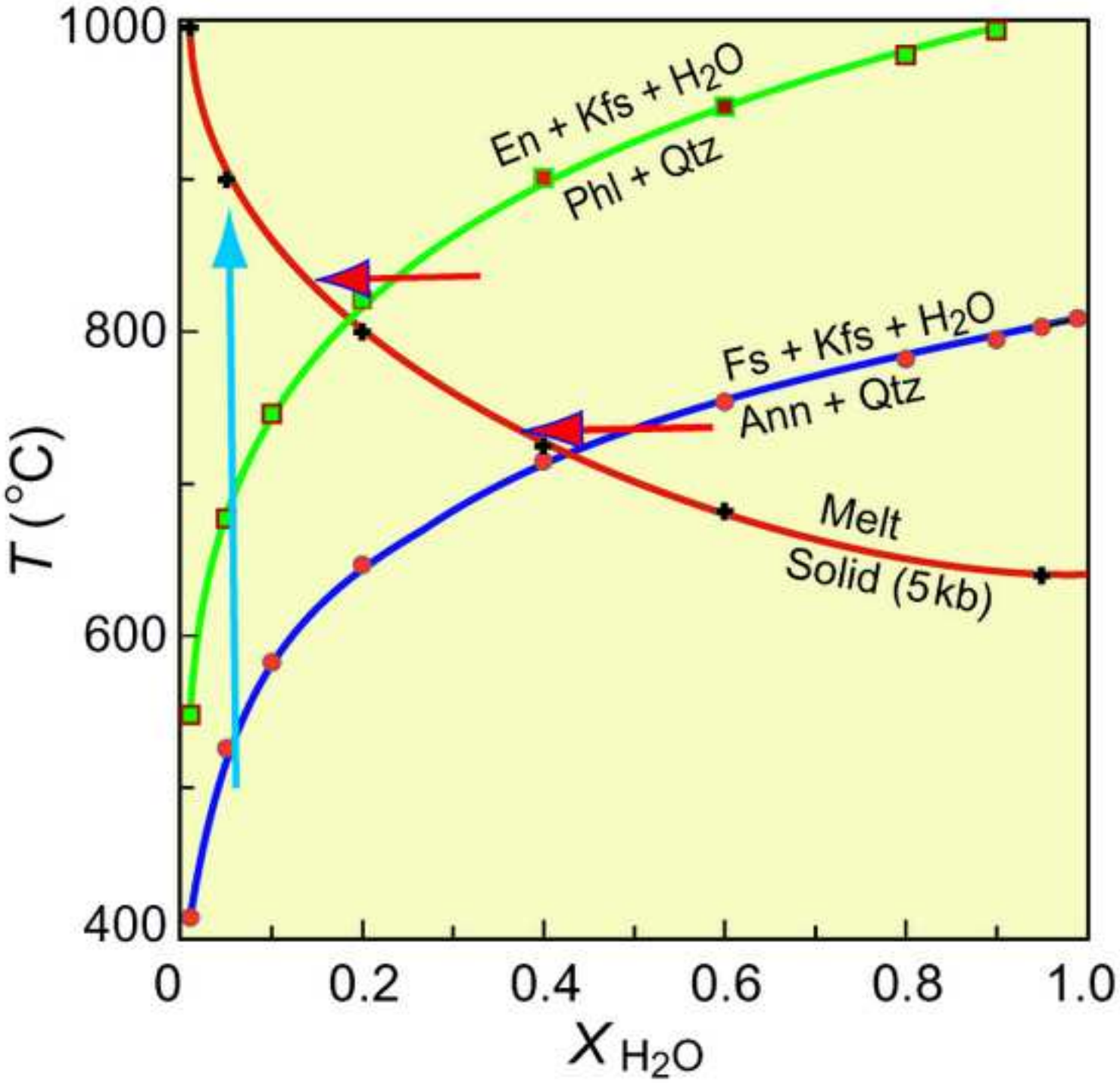

Figure 11

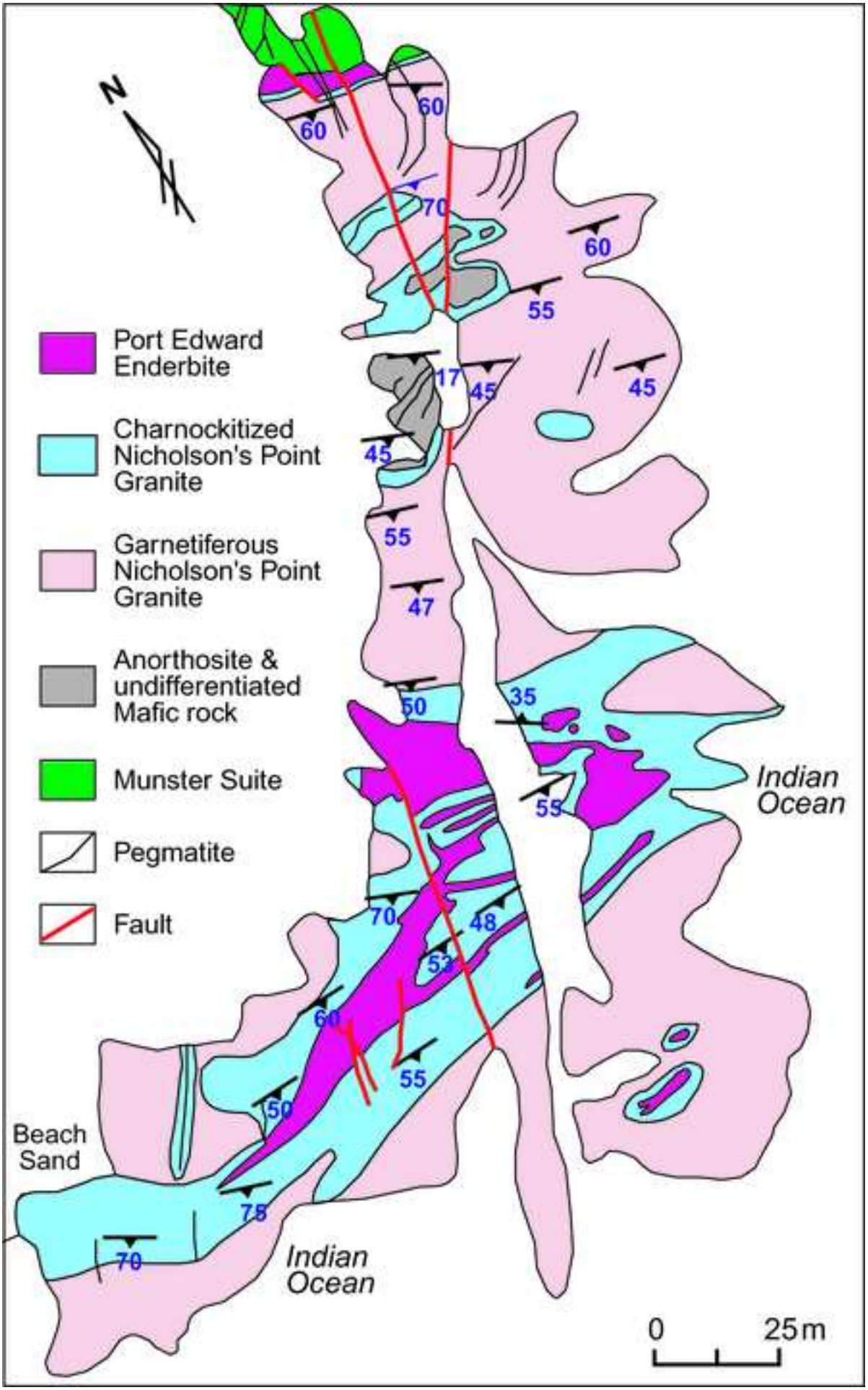

Figure 12

Click here to download high resolution image

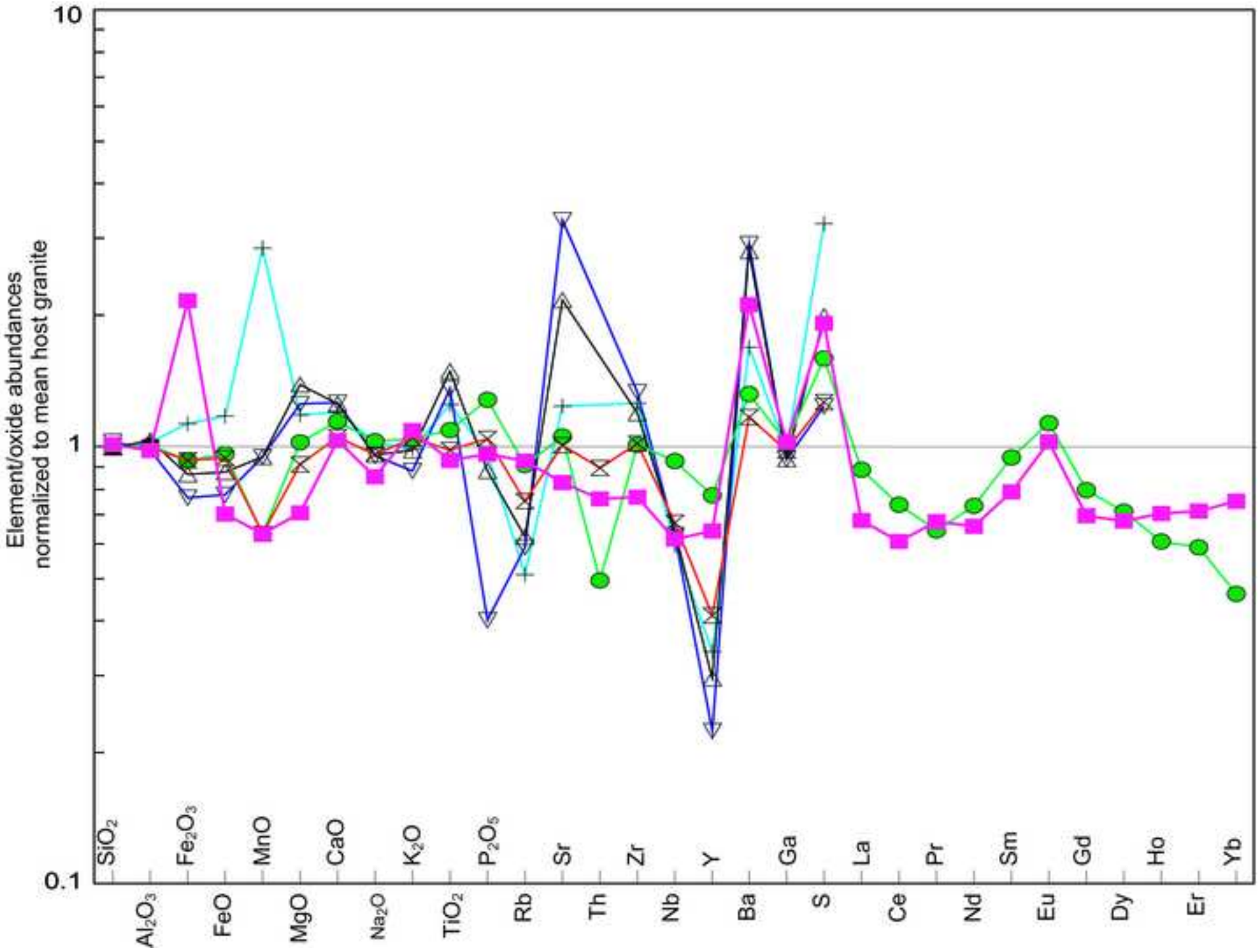

Figure 13
Click here to download high resolution image

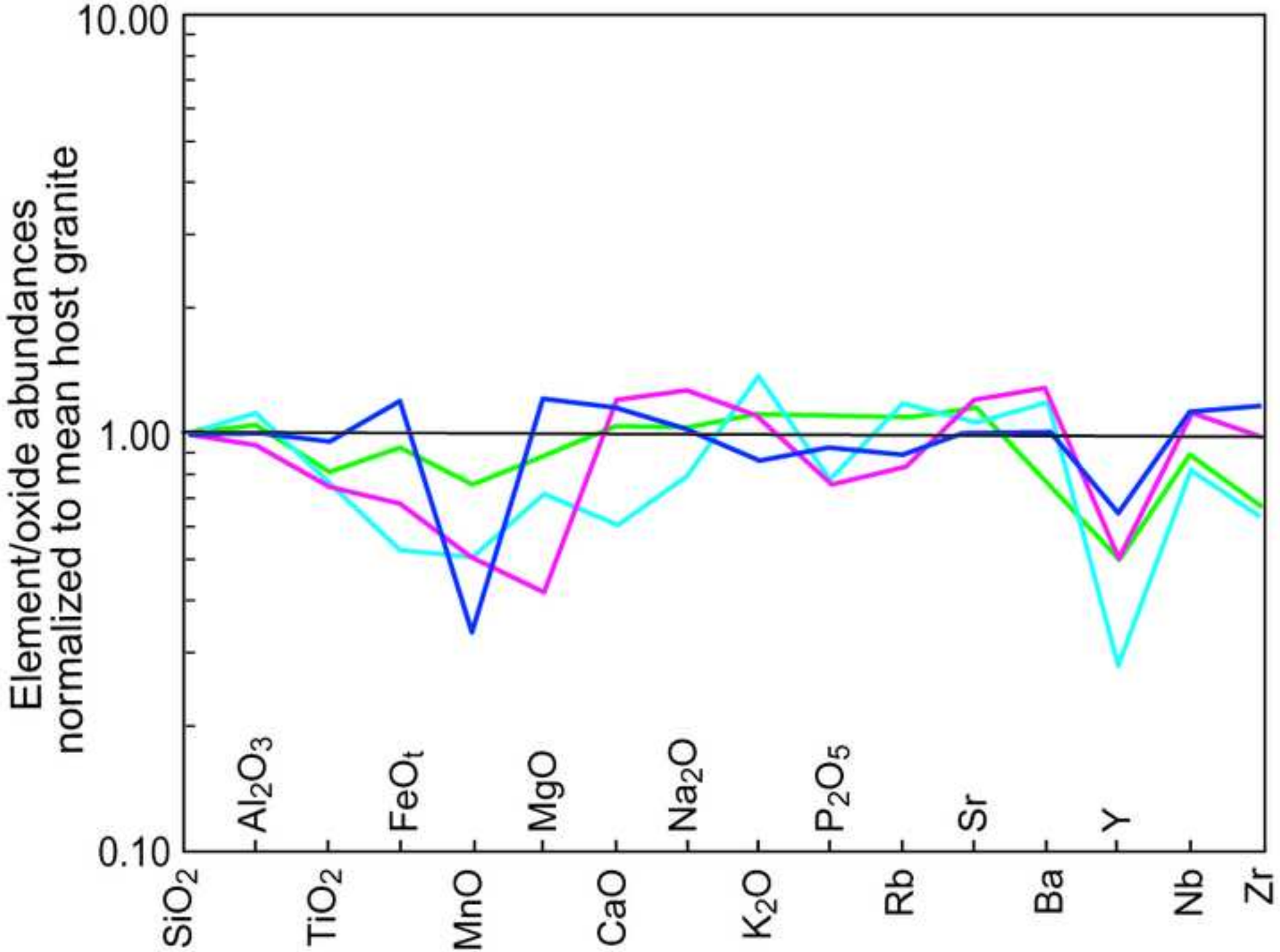

Table 1 Major and trace element chemistry from the Port Edward pluton of the Oribi Gorge Suite. Major elements are in wt.% whereas trace elements are in ppm.

	GG75	GG67	GG71	GG74	UND4	UND3	GG83	RG5	UND2	UND5	UND1	RG4	GG85	GG97	GG86
SiO_2	52.66	53.65	55.54	55.68	55.76	56.3	57.08	57.71	57.78	59.39	59.67	60.3	61.88	62.14	63
Al_2O_3	16.55	16.15	15.98	15.53	15.37	15.45	15.57	14.68	14.62	15.58	15.65	14.45	14.72	14.99	15.52
Fe_2O_3	2.59	2.46	2.38	2.46	2.45	2.39	2.39	2.40	2.34	2.18	2.13	2.46	1.88	1.93	1.85
FeO	9.21	9.58	8.47	8.67	8.62	8.30	7.77	7.74	8.07	7.15	6.95	6.81	6.08	6.28	4.48
MnO	0.18	0.18	0.17	0.17	0.17	0.15	0.15	0.11	0.15	0.13	0.13	0.13	0.11	0.12	0.09
MgO	3.08	3.10	2.71	2.60	2.53	2.46	2.42	2.24	2.23	2.00	1.89	2.17	1.66	2.06	1.38
CaO	6.53	6.57	5.80	6.00	5.95	5.77	5.68	5.28	5.26	4.88	4.90	3.65	4.78	4.21	3.23
Na_2O	3.26	3.51	3.31	3.11	3.00	2.94	3.31	3.17	2.85	2.91	3.02	2.25	3.24	2.92	2.43
K_2O	2.14	1.24	2.16	2.42	2.59	2.72	2.90	3.08	2.88	3.28	3.23	5.22	3.14	3.35	6.44
TiO_2	2.73	2.72	2.57	2.43	2.41	2.35	2.19	2.16	2.22	1.96	1.84	1.50	1.68	1.51	0.95
P_2O_5	1.04	1.06	1.01	0.93	0.93	0.89	0.84	0.82	0.79	0.74	0.69	0.54	0.61	0.50	0.33
Total	99.97	100.22	100.10	100	99.78	99.72	100.30	99.39	99.19	100.20	100.10	99.48	99.78	100.01	99.70
Rb	53	25	42	43	52	55	58	74	55	69	72	117	68	71.8	144
Y	83	100	74	76	73	72	71	80	69	66	64	49	70	59.2	38
Nb	26	29	30	22	21	22	19	22	23	20	20	14	18	18.7	8
Sc	30	35	29	33	29	29	24	29	27	26	21	24	25	24	19
La	69	66	65	59	57	66	66	77	68	64	66	25	78	65.1	40
V	128	131	118	111	110	110	100	96	102	90	85	105	86	80.1	56
Sr	429	478	548	509	499	478	527	442	446	456	429	512	406	322	487
Zr	572	572	479	544	528	522	499	595	666	565	572	376	534	495	455
Ba	1184	483	1178	1343	1187	999	1337	1153	1115	1179	1106	2671	1065	1111	2247
Cr	24	29	58	21	17	52	19	47	17	16	12	39	28	37.9	8
Cu	10	13	10	14	13	12	11	13	11	9	9	8	8	10.7	37
Ni	10	9	21	9	6	15	7	14	5	6.6	4	5	8	12	9
Zn	193	197	187	180	177	180	157	161	177	157	155	153	142	131	103

Table 2 Tabulation of data from the stable isotope analysis of fluids released during decrepitation experiments on samples from the Port Edward pluton and Oribi Gorge plutons of the Oribi Gorge Suite.

Results showing the carbon isotopic composition of fluid inclusions in charnockites					
Sample Nos.	Sample type	Decrepitation temperature (°C)	CO_2 gas released (mmol/g)	$\delta^{13}C_{PDB}$	1σ
GG-67 (Port Edward pluton)	Quartz	800	19.30	−7.99	0.03
	Whole rock	800	25.70	−6.82	0.02
	Whole rock	1000	38.42	−9.72	0.03
	Whole rock + V_2O_5	1000	34.17	−10.15	0.01
UM-2 (Oribi Gorge pluton)	Quartz	800	6.97	−1.1	0.04
	Whole rock	800	14.51	−5.61	0.01
	Whole rock	1000	15.83	−6.15	0.01
	Whole rock + V_2O_5	1000	16.39	−6.94	0.02

1

Table 3 Major and trace element chemistry from the Portobello granite. Major elements are in wt.% whereas trace elements are in ppm.

	Charnockite								Pink granite							
	PB1	PB2	PB3	PB4	PB11	PB13	PB14	PB16	PB5	PB6	PB7	PB8	PB15	PB12	PB17	PB18
SiO_2	68.12	71.22	71.17	71.43	72.66	72.83	70.99	69.33	71.94	70.93	71.67	70.46	72.19	73.15	71.60	71.96
Al_2O_3	14.59	14.40	13.72	14.01	14.36	14.17	14.02	14.95	13.15	13.63	13.93	14.51	13.82	13.82	13.69	13.82
Fe_2O_3	3.21	2.20	1.71	2.06	1.84	1.83	2.27	3.17	1.90	2.16	1.88	2.11	1.98	1.75	2.21	2.22
FeO	0.40	0.27	0.21	0.25	0.23	0.23	0.28	0.39	0.24	0.27	0.23	0.26	0.24	0.22	0.27	0.27
MnO	0.01	0.01	0.01	0.02	0.02	0.03	0.02	0.04	0.02	0.03	0.01	0.02	0.02	0.02	0.02	0.03
MgO	0.92	0.55	0.41	0.57	0.62	0.61	0.64	0.84	0.53	0.54	0.50	0.56	0.48	0.42	0.52	0.50
CaO	2.64	1.73	1.45	1.51	1.96	1.68	1.21	2.53	0.86	1.11	1.12	0.81	0.98	1.05	1.19	0.90
Na_2O	3.53	3.44	2.77	3.64	2.74	2.61	2.24	3.00	3.49	3.08	3.09	3.63	2.20	2.38	2.13	2.33
K_2O	4.20	4.88	6.50	4.93	4.64	5.04	6.34	3.95	5.36	6.06	5.88	5.60	6.31	6.03	6.23	6.24
TiO_2	0.51	0.30	0.32	0.28	0.36	0.31	0.47	0.55	0.40	0.34	0.38	0.40	0.39	0.28	0.43	0.40
P_2O_5	0.19	0.12	0.25	0.12	0.11	0.10	0.28	0.15	0.16	0.23	0.22	0.23	0.19	0.13	0.23	0.20
LOI	1.10	0.73	0.01	0.56	0.12	0.22	0.46	0.38	1.22	1.12	0.88	0.97	0.56	0.39	0.64	0.68
Total	99.41	99.85	98.53	99.38	99.66	99.66	99.22	99.28	99.27	99.50	99.79	99.56	99.36	99.64	99.16	99.55
Rb	130	148	204	157	149	147	178	125	173	212	181	208	174	183	201	203
Sr	499	208	296	190	377	334	230	469	284	131	267	221	188	162	152	130
Ba	1779	1204	820	1014	843	842	582	1546	785	501	686	705	532	605	517	451
Y	11	12	17	11	7	6	20	10	17	27	23	27	15	14	25	43
Nb	8	7	12	9	6	7	11	7	15	12	15	15	11	9	13	14
Zr	397	213	245	202	246	213	329	410	302	261	271	284	274	187	299	274
Sc	9	5	5	4	4	4	4	6	6	4	8	5	3	3	3	3
Ga	20	18	20	19	20	19	20	21	18	16	19	21	19	20	21	20
V	30	16	7	13	38	32	39	55	17	10	13	13	34	27	40	35
Cu	11	8	10	7	5	5	6	5	7	9	8	9	7	5	5	5
Ni	3	5	3	6	5	5	5	5	7	3	3	3	5	5	5	5
Zn	56	48	30	41	41	36	50	62	36	45	37	44	39	40	53	41